0 0 0 0 4 9 0 1 2 3 6

LBL-6852 c.1
UC-59
TID-4500-R66

RECEIVED
LAWRENCE
BERKELEY LABORATORY

MAR 8 1978

LIBRARY AND
DOCUMENTS SECTION

For Reference

Not to be taken from this room

Energy and Environment Division

Application Of Turbomachinery In Solar-Assisted Rankine Cooling Systems

John Leech

December 14, 1976

Lawrence Berkeley Laboratory University of California/Berkeley

Prepared for the U.S. Department of Energy under Contract No. W-7405-ENG-48

LBL-6852 c.1

LEGAL NOTICE

This report was prepared as an account of work sponsored by the United States Government. Neither the United States nor the Department of Energy, nor any of their employees, nor any of their contractors, subcontractors, or their employees, makes any warranty, express or implied, or assumes any legal liability or responsibility for the accuracy, completeness or usefulness of any information, apparatus, product or process disclosed, or represents that its use would not infringe privately owned rights.

Printed in the United States of America
Available from
National Technical Information Service
U. S. Department of Commerce
5285 Port Royal Road
Springfield, VA 22161
Price: Printed Copy, $ 5.25 Domestic; $10.50 Foreign
Microfiche, $ 3.00 Domestic; $ 4.50 Foreign

0 0 0 0 4 9 0 1 2 3 7

BARBER-NICHOLS ENGINEERING

APPLICATION OF TURBOMACHINERY

IN

SOLAR-ASSISTED RANKINE COOLING SYSTEMS

December 14, 1976

Prepared for:

John Leech
Energy Research and
Development Administration
Washington, D.C.

and

Lawrence Berkeley Labs
University of California
Berkeley, California

Prepared by:

Barber-Nichols Engr. Co.
Arvada, Colorado

Work performed under the auspices of the U. S. Department of Energy.

6325 West 55th Avenue, Arvada, Colorado 80002 Telephone 303-421-8111

0 0 0 0 4 9 0 1 2 3 8

TABLE OF CONTENTS

		Page
1.0	INTRODUCTION	1
2.0	SUMMARY	1
3.0	VAPOR COMPRESSOR MATCHING	3
	3.1 CYCLE CONDITIONS	3
	3.2 COMPRESSOR OPERATING CHARACTERISTICS	4
4.0	AXIAL FLOW TURBO-EXPANDER CONCEPTS	4
	4.1 SINGLE AND MULTI-STAGE AXIAL FLOW TURBINES	5
	4.1.1 Turbine Description	5
	4.1.2 Performance Evaluation	5
	4.1.2.1 Assumptions	5
	4.1.2.2 Method of Evaluation	9
	4.1.2.3 Determination of Losses	11
	4.1.3 Results	12
	4.2 LOW SPECIFIC SPEED STAGING	12
	4.2.1 Axial Turbine Stages	12
	4.2.2 Drag or Terry Turbines	15
	4.3 LOW VOLUMETRIC FLOW TURBINE	15
	4.3.1 Description	17
	4.3.2 Estimated Performance	17
5.0	RADIAL OUTFLOW SINGLE DISC TURBINE	21
	5.1 TURBINE DESCRIPTION	21
	5.2 PERFORMANCE EVALUATION	21
	5.2.1 Assumptions	21
	5.2.2 Method of Evaluation	22
	5.2.3 Determination of Losses	25
	5.2.4 Overall Turbine Performance	26
	5.3 TURBINE PERFORMANCE EVALUATION	27
6.0	CONCLUSIONS	27
7.0	REFERENCES	29
	APPENDIX	30

1.0 INTRODUCTION

This report presents the results of a preliminary study concerning the use of high speed turbomachinery in a solar-assisted Rankine cooling cycle. The use of Rankine cycles in solar powered cooling of buildings involves a solar collector to provide energy to heat and vaporize a working fluid. Energy is extracted from this vapor in an expansion engine that is used to drive an air conditioning vapor compressor. In a typical Rankine cycle, the maximum temperature at the inlet to the expander is limited to the temperature of the fluid leaving the solar collector. Because of the relatively low temperature capability associated with inexpensive collectors the efficiency of the Rankine cycle is generally low. This low efficiency results in low coefficient of performance values for the solar powered cooling system.

In an effort to improve Rankine cycle efficiency, a solar-assisted approach was presented in NSF report RA-N-75-012, by Dr. Henry Curran. In this approach solar energy vaporizes the working fluid at a low temperature using solar collectors; the vapor is subsequently superheated to a higher temperature using fossil fuel, thereby allowing the potential of much improved Rankine cycle efficiency as compared to a typical cycle. Water was selected as the working fluid to avoid problems associated with chemical stability of organic fluids at high values of expander inlet temperature. A maximum steam temperature of 1100°F was suggested to achieve Rankine cycle efficiencies on the order of 25%. The solar-assisted Rankine cycle was shown by Dr. Curran to offer a substantial cost advantage over conventional absorption machinery. Key elements in achieving this performance improvement are the efficiency of the Rankine cycle vapor expander and the performance of the vapor cycle. In Dr. Curran's study, an expander efficiency of 82% and an air conditioning COP_{VC} of 4.0 was assumed. Additionally, no losses were included for drive efficiency, implying a direct drive between the vapor expander and the air conditioning compressor.

The intent of the present study was to identify the performance potential of practical turbine expanders and vapor compressors, and provide preliminary definition of the hardware. The remainder of this report presents the results obtained during this study.

2.0 SUMMARY

A variety of turbo-expanders were considered for use in the solar-assisted Rankine cooling system. Among these were : 1) single and multi-stage, pressure-compounded, axial flow turbines; 2) multi-row, single disc. radial flow turbines; 3) turbines favoring low specific speed, such as velocity staging, and advanced turbine concepts such as high reaction, partial admission turbine stages.

The potential performance of these turbine concepts was estimated using empirical correlations verified by years of testing and turbine performance evaluation by Barber-Nichols. The non-dimensional coefficients of

specific speed (Ns), specific diameter (Ds), Mach number (M'), and Reynolds number (Re) were used to estimate potential efficiency and losses associated with each concept. Performance was examined over a range of power levels from 1 hp to 75 hp, and at speeds consistent to match the characteristics of the vapor compressor. This power level corresponds to the cooling cycles of Dr. Curran's townhouse cooling (1 hp) and to the recent NASA-Marshall RFP's (up to 75 tons).

The basic concept involves the use of auxiliary fuel to obtain a higher maximum temperature than can be achieved with available low cost collectors. This higher temperature allows higher Rankine cycle efficiency because of the greater temperature difference between the maximum and sink temperatures. Fluid conditions selected for the present study were:

Maximum steam temperature	1100°F
Saturated collector temperature	320°F
Condensing temperature	120°F

The absolute values of cooling loads and efficiencies calculated herein are strictly applicable only for the selected cycle conditions. General conclusions reached as a result of the study may be considered valid for any high temperature steam Rankine cycle at the levels of output power examined.

The high steam temperature and the specified cycle conditions result in a steam available energy to the turbine of 448 Btu/lb. The effect of the high energy level on turbine design and performance is two-fold. First, in order to efficiently convert the energy to shaft power, a high turbine blade speed related to the available energy is required. Approximately 2-4 pressure compounded stages are necessary to avoid damaging stress levels at turbine blade speeds consistent with optimum turbine stage performance. The second consideration involves turbine flow rate. For example, for one net horsepower and assuming an overall efficiency of 60%, the turbine flow rate is 9.5 lb/hr of steam. This low flow rate and the high steam energy and velocity result in low values of turbine stage specific speed. Specific speed was used as the correlating performance parameter since it relates optimum achievable performance to design variables, such as passage size, blade height, and arc of admission. Additionally, years of correlating experience have verified the applicability of this parameter in estimating overall performance of the turbine concepts considered in this study.

Values of turbine efficiency (.82) and COP_{VC} (4.0) used in Dr. Curran's report in evaluating the solar-assisted Rankine cycle were found to be reasonable at levels of cooling capacity greater than about 20 tons. Below this capacity, turbine efficiency falls off because of practical limitations which prevent optimum aerodynamic configurations as discussed above. Conventional turbine stages in the range of 1-3 hp operating at the above speeds would achieve a maximum efficiency of from 50- 62% and require 4-6 pressure compounded stages. An advanced turbine concept could be utilized to achieve maximum efficiencies on the order of 70%, but extensive development effort would be required since this concept is presently of unproven design. Multi-blade row

single disc turbines may eventually offer a cost advantage over complex axial flow turbines; however, in every case examined during this preliminary study, a performance penalty, as compared to the axial flow turbines, was indicated. Estimated vapor compressor efficiencies ranged from 65 to greater than 70% for cooling capacities of 1-75 tons. Compressor considerations also show optimum rotational speeds of 50,000-80,000 rpm for the turbocompressor.

In conclusion, the solar-assisted Rankine cycle can offer substantial performance advantage over saturated or low temperature cycles. Care must be exercised, however, in selecting the power level and area of applicability in order to achieve acceptable levels of performance of the rotating machinery.

3.0 VAPOR COMPRESSOR MATCHING

The vapor compressor component is an important element in the solar-assisted cooling cycle. Compressor efficiencies in the range of 70% are required to achieve the value of COP_{VC} (4.0) reported in Reference 1. Additionally, in order to avoid power losses associated with typical speed reducers, it is desirable to operate the vapor compressor at the same rotational speed as the turbine. Since the compressor generally favors a lower rotational speed than the turbine, the individual performance characteristics of these components must be considered in selecting the rotational speed of the turbocompressor unit. Barber-Nichols has designed and tested several high speed vapor compressors operating on R-113 at 2-3 tons cooling capacity. These units operated in the range of 50,000 rpm, and efficiencies greater than 70% were achieved at pressure ratios of about 7:1. These data were used to bracket the vapor compressor performance in this study.

The following section describes a brief analysis performed to determine the suitability of direct coupling the vapor compressor to the expander in the solar-assisted Rankine cycle and to evaluate the overall effect on system performance.

3.1 CYCLE CONDITIONS

A 45°F evaporator and a 120°F condenser were selected for the air conditioning cycle (Ref. 1). An ideal horsepower per ton (.81) was calculated for several working fluids and a compressor efficiency of .68-.70 was estimated to achieve COP vapor cycle = 4.0 and a required input power to the vapor compressor of 1.2 hp/ton. This value can be used to convert delivered turbine horsepower to nominal system cooling capacity.

The optimum refrigerant selected for any given application is a function of cooling capacity and desired operating characteristics. For values of cooling capacity less than about 10 tons and utilizing a centrifugal compressure, R-113 is generally considered a good candidate fluid. Increased capacity generally favors fluids such as R-11. These fluids were used to estimate volumetric flow rates and capacities for the centrifugal compressor

in the air conditioning system.

3.2 COMPRESSOR OPERATING CHARACTERISTICS

Based on Barber-Nichols' previous experience, overall compressor efficiency can be estimated using compressor specific speed as a correlating parameter. For purposes of this study, specific speed was based on inlet volume flow:

$$N_S = \frac{N \sqrt{Q}}{(\Delta H_S)^{3/4}}$$

where N = rotational speed, rpm
Q = volumetric flow rate, ft^3/sec
ΔH_S = isentropic head rise, ft

Values of specific speed of from 80-120 are required in order to achieve optimum efficiencies. Values of compressor capacity of from 1-75 tons were examined. At low power levels, in the range of 3-10 hp, compressor speeds in the range of 50-80,000 rpm can be utilized to achieve efficiencies in the range of 70-75%. Below 3 hp, compressor size and Reynolds number effects combine to lower efficiency to the range of 65-70% at a similar speed range. At a capacity of 75 tons, the optimum compressor speed was calculated to be 30-40,000 rpm. The optimum speed can be increased, however, to about 60,000 rpm by utilizing a double inlet to the centrifugal compressor or axial flow compressor stages.

In conclusion, over the range of cooling loads examined, a direct coupled compressor, operating at rotational speeds of from 50-80,000 rpm can achieve acceptable performance levels to maintain a COP_{VC} of 4.0 at 120°F condensing temperature. Appropriate selection of refrigerant and detail design of the compressor will be dependent on the cooling capacity and required system operating characteristics.

4.0 AXIAL FLOW TURBO-EXPANDER CONCEPTS

The steam expanders considered in this report were limited to high speed turbomachinery. Lower speed positive displacement machinery has also been discussed for use in high temperature steam engines. Development problems associated with reliability and performance, and limited expansion ratios are felt to preclude consideration of these engines in the solar-assisted cycle. Steam turbines have been used for years at similar steam conditions and a wealth of information is available from which design constants and material selections can be obtained. A variety of axial flow turbo-expanders were considered for use in the solar-assisted Rankine cooling cycle. Single and multi-stage axial flow turbines generally represent years of development. The predicted levels of performance should be considered achievable with a relatively small amount of development. Other turbine concepts considered in this section of the report include velocity

compounded stages and a unique low volumetric flow turbine.

A detailed assessment of turbine costs were beyond the scope of the present study. General comments relating to relative costs and required development effort are found in respective sections of this report dealing with the specific turbine concepts.

4.1 SINGLE AND MULTI-STAGE AXIAL FLOW TURBINES

4.1.1 Turbine Description

The turbine evaluated was a conventional axial flow turbine containing from 1-6 pressure compounded stages. Figure 1 shows a typical axial flow turbine stage.

4.1.2 Performance Evaluation

The cycle evaluated was a solar-assisted Rankine cycle operating between a maximum steam temperature of 1100°F and a condensing temperature of 120°F. The saturated collector temperature was 320°F. Conventional axial flow turbines were evaluated over a wide range of speeds, horsepower levels, and stage numbers as shown in Table I.

4.1.2,1 Assumptions

Prior to proceeding with any calculations, a number of assumptions had to be made because of the interrelationship between a large number of parameters. For example, the efficiency of each stage is affected by the head drop across each stage and this, in turn, affects the overall efficiency and performance of the turbine.

The primary assumption made was that the head drop was equal across each stage. Based on previous experience in calculating turbine performance the final efficiency with optimized head drop per stage is very close to that calculated with equal head drop per stage. In addition, this assumption generally allows nearly constant wheel diameter for the stages since the optimum efficiency is related to the rotor blade speed divided by the available energy. The last stage head drop was corrected to insure that the steam expanded to the exit pressure of 1.7 lb/in^2, absolute, corresponding to 120°F condensing.

A second assumption was that the rotor tip speed was limited to 1500 feet per second. This speed limitation was made to avoid damaging stress levels associated with very high blade speeds.

A third assumption was that turbines with specific speeds less than 45 were partial admission and turbines with specific speeds greater than 45 were full admission. As can be seen from Figure 2, this assumption increased the diagram efficiency for turbines with specific speeds less than 10 and also improved the efficiencies by about 3-6% for turbines with specific speeds of

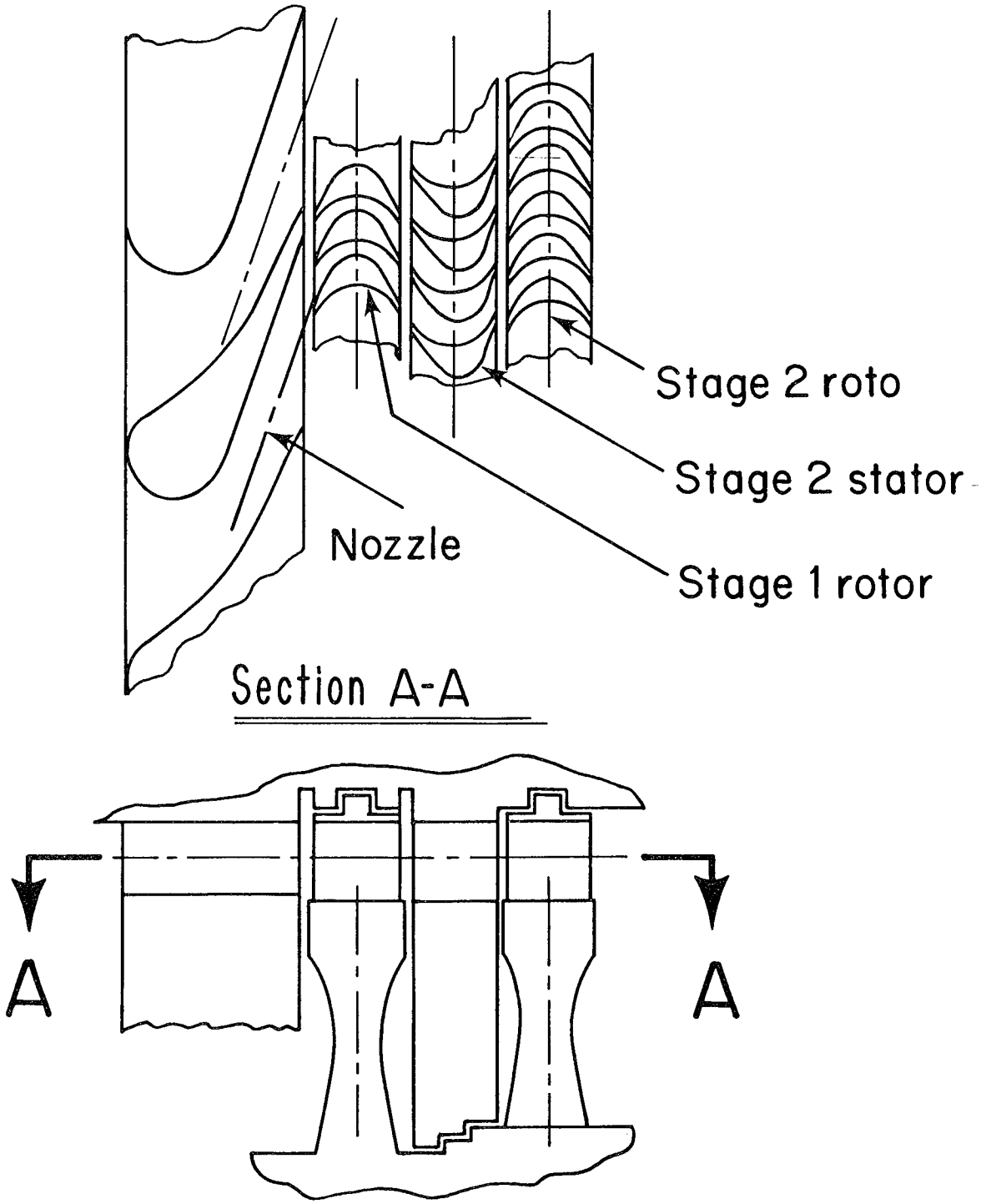

XBL 7711-11400

Fig. 1 Typical Axial Flow Turbine Stage

TABLE I

SUMMARY OF AXIAL FLOW TURBINE EFFICIENCY

	HORSEPOWER					
	1		25		75	
Stages	rpm	η_t	rpm	η_t	rpm	η_t
1	-	-	-	-	25K	59.7%
1	50K	38.3%	-	-	50K	58.9%
1	-	-	75K	57.0%	75K	58.4%
1	-	-	90K	56.1%	-	-
1	150K	34.8%	150K	55.2%	150K	46.6%
2	-	-	-	-	50K	75.5%
2	-	-	75K	72.6%	-	-
2	-	-	90K	73.3%	90K	73.6%
2	-	-	150K	75.1%	-	-
4	-	-	-	-	50K	79.1%
4	75K	55.3%	-	-	75K	82.7%
4	150K	57.9%	-	-	150K	77.9%
6	-	-	75K	79.6%	-	-
6	90K	54.9%	90K	81.2%	-	-
6	150K	57.7%	150K	82.3%	-	-

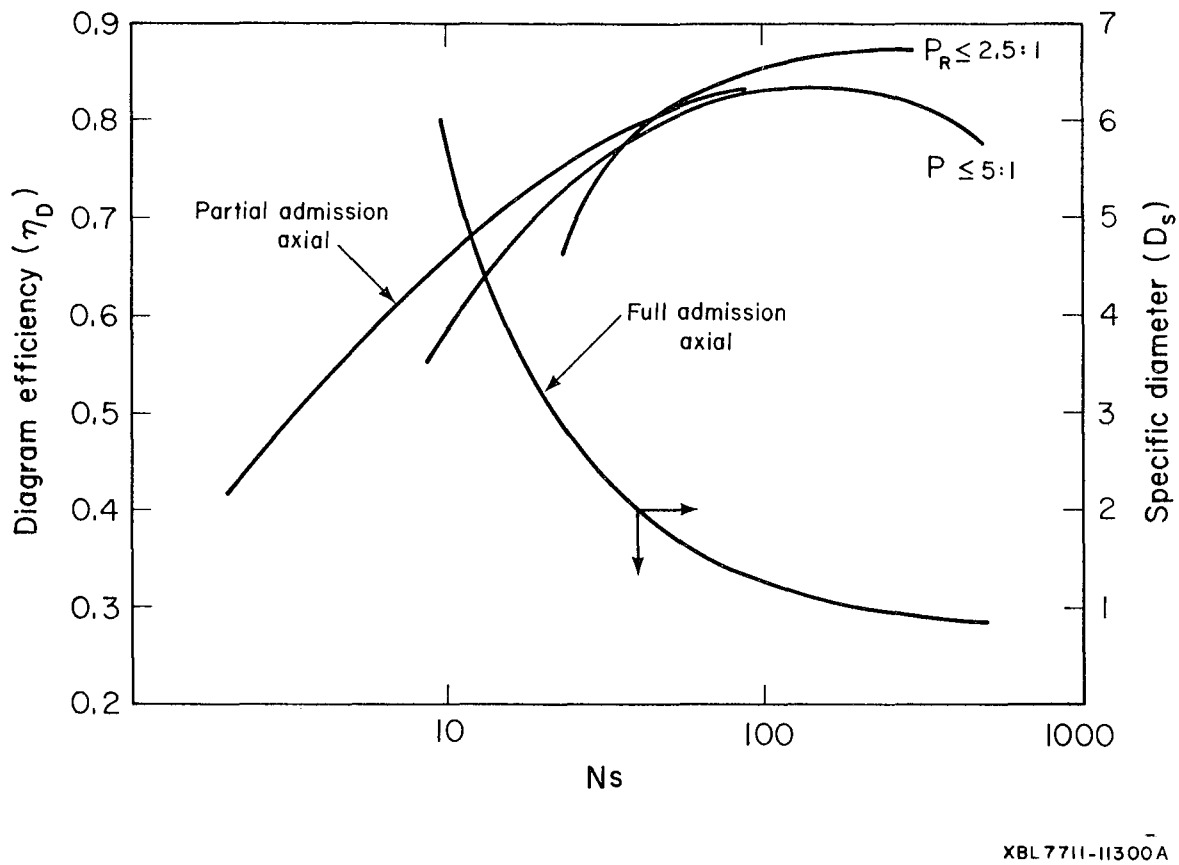

Fig. 2 Diagram Efficiency and Specific Diameter vs. Specific Speed

10-25. The improved turbine efficiency for partial admission turbines is the result of improved flow passages in the turbine blading. In general, low values of turbine specific speed correspond to low volumetric flow rates. Continuity of flow must be conserved in high efficiency blading, and low specific speed stages consequently have typically small blade passage areas. As blades become extremely short, blading efficiency suffers. This problem is alleviated in partial admission turbines since, as the name implies, flow is admitted over a portion of the turbine periphery and the blading can be made correspondingly larger and more efficient. Not all the improved blading efficiency is realized, however, since partial admission turbines have other characteristic losses. These losses are termed scavenging and blade pumping loss, and represent flow losses occurring in the unadmitted turbine arc. Disc windage, blade pumping, and scavenging losses have previously been estimated as a function of turbine specific speed (Ref. 2), and are included in the diagram efficiency.

4.1.2.2 Method of Evaluation

To evaluate the performance of the turbines listed in Table I, the horsepower output desired, speed in revolutions per minute, and number of stages were selected. The overall isentropic drop in head between the pressure of the superheated steam (89.7 psia) and the condensing pressure (1.7 psia) was evaluated from the Mollier diagram. To start the performance calculations, an overall turbine efficiency based on past experience was assumed. This overall efficiency with the selected horsepower and the overall isentropic head drop was used to calculate a turbine mass flow rate from the equation

$$\dot{w} = \frac{HP\ (550)}{\eta_T\ \Delta H'_{id}\ (778)}$$

where $\dot{w}$ is in lbm/sec.

The isentropic head drop per stage was then calculated from the equation

$$\Delta H'/\text{stage} = \frac{R\ \Delta H'_{id}}{n}$$

where n is the number of stages and R is the reheat factor determined from the equation

$$R = 1 + (R_\infty - 1)(1 - \frac{1}{n})(\frac{1 - \eta_s}{0.2}) \quad \text{(Ref. 3)}$$

where R_∞ is the reheat factor for an infinite number of stages of 80% stage efficiency and η_s is the stage efficiency of the turbine under evaluation.

The estimated value of $\Delta H'$ per stage and an estimated stage efficiency were then used to calculate an exit enthalpy for the first stage. The estimated

$\Delta H'$ per stage was also used to determine an exit pressure from the Mollier diagram. The exit pressure and exit enthalpy were then used to determine an exit specific volume for the first stage from the steam tables. This exit specific volume along with the turbine mass flow rate was then used to determine the stage volume flow rate in ft^3/sec from the equation

$$Qe = \upsilon e \, \dot{w}$$

There are four similarity parameters, specific speed (Ns), specific diameter (Ds), machine Reynolds number (Re*), and Mach number (M'), that can be derived from a technique known as dimensional analysis, and can be used as convenient parameters for presenting the performance criteria of turbomachines. These four parameters along with rotor tip speed, rotor diameter, and ratio of rotor tip speed-to-isentropic spouting velocity were then calculated for the first stage using the following equations

$$Ns = \frac{N \sqrt{Qe}}{(\Delta H' id_s J)^{3/4}}$$

$$U = \left(\frac{U}{C_o}\right) \left(\sqrt{2g \, J \, \Delta H's}\right)$$

$$Dia. = \frac{U \, (720)}{\pi \, N}$$

$$\frac{U}{C_o} = \frac{Ns \, Ds}{154}$$

and

$$Re^* = \frac{U \, Dia \, \rho}{12 \, \mu}$$

where

Ns	=	specific speed
Ds	=	specific diameter
N	=	rotor rpm
J converts Btu/lbm to ft-lb/lbm		
U	=	rotor tip speed
g	=	32.2 ft/sec^2
C_o	=	isentropic spouting velocity
Dia.	=	rotor diameter
ρ	=	the exit fluid density
μ	=	the exit fluid viscosity

The values of specific diameter (Ds) and diagram efficiency (η_D) were determined from Figure 2. The Mach number (M') was determined from the Mach tables at $\gamma = 1.3$, using the pressure ratio across the stator.

4.1.2.3 Determination of Losses

A number of efficiency corrections, or losses, were evaluated. They included a correction for rotor tip speed if the rotor tip speed of a stage exceeded 1500 ft/sec, a correction for machine Reynolds number (Re*) if the Reynolds number was less than 1×10^6, a leakage correction based on the equation

$$\% \text{ leakage} = \frac{C_1}{h}$$

where C_1 is the rotor shaft seal clearance and h is the rotor blade height which was determined from Balje (Ref. 2) for either partial admission or full admission stages. The above relationship was used in the majority of the calculations to obtain an estimate of the stage leakage. The values of calculated leakage are conservative; that is, greater than anticipated in an optimally designed turbine since the sealing diameter can typically be less than the turbine rotor diameter, and staggered labyrinths can often be used to reduce seal flow coefficients. A detailed stage performance evaluation including optimized seal configuration would have required substantially more effort than was felt to be necessary to meet the goals of the present study. Where leakage losses were seen to have a significant influence on the conclusions of the study, a more detailed evaluation of stage leakage is provided. A Mach number correction was also included if the rotor inlet relative Mach number was greater than unity. The rotor inlet relative Mach number (AMR) was determined from the equation

$$AMR = 0.94\,(1-U/C_o)M'$$

where 0.94 is a function of the nozzle angle α and the nozzle velocity coefficient ψN.

4.1.2.4 Overall Turbine Performance

To evaluate the overall efficiency of the stage, the diagram efficiency obtained from Figure 2 was multiplied by the losses to obtain an overall stage efficiency η_s, using the following equation

$$\eta_s = \eta_D\,(\eta/\eta_D\,(U/C_o))\,(\eta/\eta_D\,(Re^*))\,(\eta/\eta_D\,(AMR))\,(1\text{-leakage fraction})$$

where $\eta/\eta_D\,(U/C_o)$ is the correction for rotor tip speed $>$ 1500 ft/sec

$\eta/\eta_D\,(Re^*)$ is the Reynolds number correction

$\eta/\eta_D\,(AMR)$ is the inlet relative Mach number correction

(1-leakage fraction) is the leakage correction that applied to all but the first stage.

The calculated stage efficiency (η_s) was then used to recalculate the exit enthalpy and a head drop for the first stage. The entire procedure starting

with a new estimated stage efficiency was then repeated for all remaining stages.

The final step was to add all the head drops for the individual stages and divide them by the isentropic head drop for the turbine to obtain the overall turbine efficiency using the equation

$$\eta_T = \frac{\sum \Delta Ha_s}{\Delta H'id}$$

where ΔHa_s is the actual head drop for each turbine stage.

If the calculated turbine efficiency was markedly different from the estimated efficiency, it was necessary to recalculate the turbine efficiency starting from a new estimated turbine efficiency and new stage efficiencies.

4.1.3 Results

The results of the turbine performance evaluations are presented in Tables I and II. Table I shows the variation in turbine efficiency with stage number, horsepower output and rpm. Turbine speeds shown exceed limits for efficient compressor operation established in section 3.0, but were included for reference. Table II is the summary of the calculations for the six-stage, 90,000 rpm turbine at one and 25 horsepower. Detailed calculations for these two turbo-expanders are presented in Appendix I.

As can be seen from Table II, the volume flow rate (Qe) for the 1 hp turbine is quite small compared to that of the 25 hp turbine. This results in a much lower specific speed, lower machine Reynolds number, and larger leakage losses as a percentage of total flow between stages. These factors all combine to lower the efficiency by approximately 32%.

Figure 3 summarizes the performance for the turbo-expanders listed in Table I. The maximum attainable overall efficiency at turbine speeds consistent with required compressor speeds (see section 3.0) is presented as a function of horsepower output and number of stages. As may be noted in the figure, values of turbine efficiency of 82% are achievable utilizing 3-6 pressure compounded stages and at output horsepowers greater than 20. At stage numbers less than three, the turbine efficiency is lower, reaching a maximum of 62% for a single stage at 75 hp. The highest efficiency calculated for one output horsepower is 59% utilizing five or six stages.

4.2 LOW SPECIFIC SPEED STAGING

4.2.1 Axial Turbine Stages

Based on the results of the analysis presented in section 4.1, the calculated specific speed (Ns) for the first turbine stages is too low ($Ns < 20$) to achieve high stage efficiency. For this reason low specific speed staging

TABLE II

MULTI-STAGE AXIAL TURBINE

Stage	Temp.	Psia	h	Qe	Ns	Ds	U/Co	Dia.	Rc*	AMR	Blade Height	% Leakage	ηs	ΔHa
6 STAGE, 1 HORSEPOWER, 90,000 RPM, $\eta_{overall}$ = 0.5490														
1	1100	89.64	1584	0.043	4.5	12.8	0.375	1.98	3.8×10^5	0.55	0.036		0.490	42.03
2	1017	52	1541.97	0.073	5.85	10.4	0.396	2.09	2.7×10^5	0.55	0.042	11.96	0.441	37.91
3	931	29.5	1498.89	0.126	7.7	8.5	0.427	2.25	1.9×10^5	0.53	0.050	10.08	0.476	40.86
4	841	16.2	1453.44	0.221	10.18	5.7	0.377	1.99	0.9×10^5	0.61	0.056	8.98	0.439	37.68
5	757	8.5	1412.03	0.419	14.02	4.2	0.382	2.02	0.5×10^5	0.62	0.071	7.07	0.442	37.98
6	673	4.25	1371.15	0.945	18.61	3.4	0.411	2.36	0.4×10^5	0.69	0.130	3.86	0.489	49.49
Exit	566	1.7	1319.65											
6 STAGE, 25 HORSEPOWER, 90,000 RPM, $\eta_{overall}$ = 0.8120														
1	1100	89.64	1584	0.916	21.27	3.1	0.428	2.22	5×10^5	0.50	0.133		0.695	57.75
2	986	53	1526.24	1.438	26.64	2.6	0.458	2.38	4×10^5	0.48	0.155	3.23	0.689	57.25
3	869	31	1467.10	2.382	34.3	2.2	0.501	2.60	3.2×10^5	0.47	0.174	2.87	0.720	59.76
4	744	17	1405.55	4.259	45.86	1.8	0.542	2.81	2.4×10^5	0.46	0.169	2.96	0.746	61.94
5	613	8.6	1341.75	7.884	62.4	1.5	0.608	3.16	1.9×10^5	0.42	0.253	1.98	0.760	63.12
6	476	4	1277.34	15.791	91.36	1.3	0.753	3.82	1.6×10^5	0.28	0.573	0.87	0.806	63.95
Exit	327	1.7	1212.75											

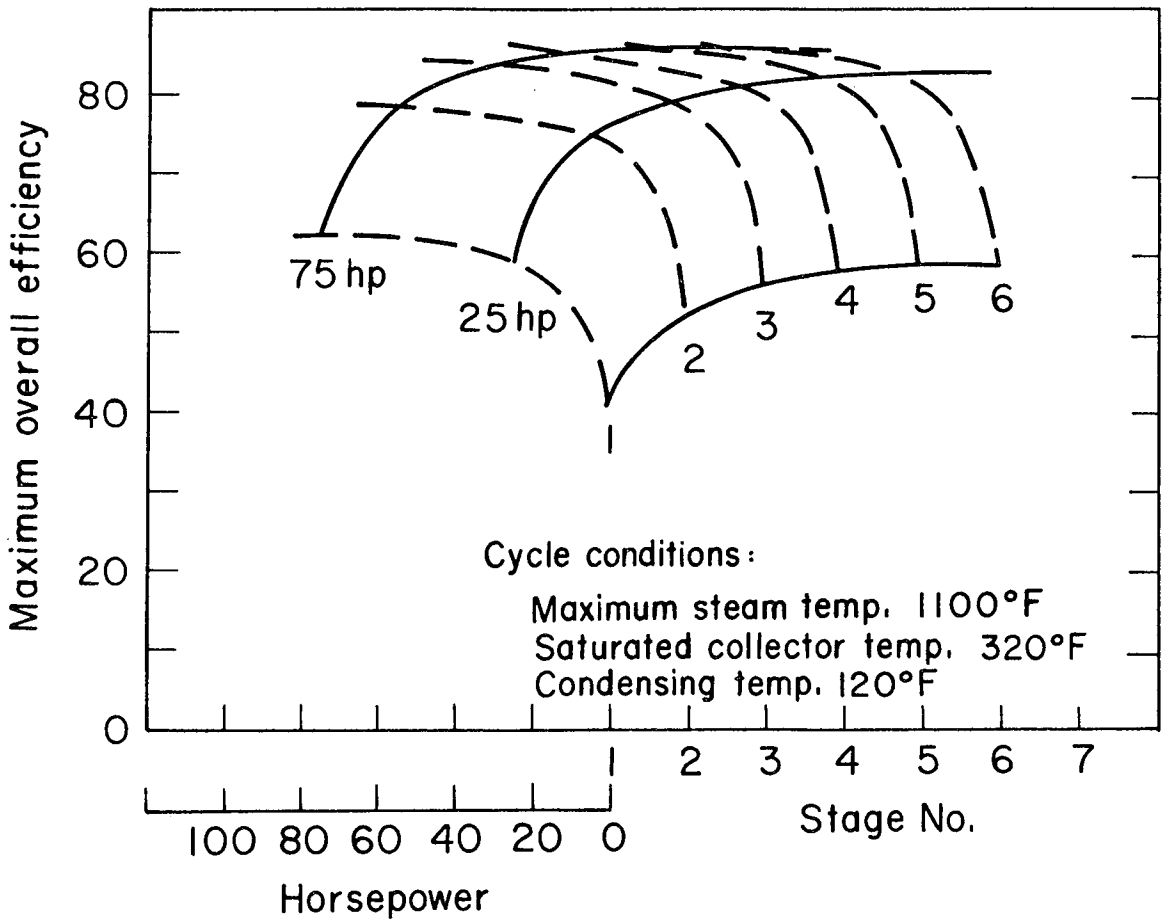

XBL7711-11303

Fig. 3 Variation of Overall Turbine Efficiency with Stage Number and Power for Axial Flow Pressure Compounded Turbines

was considered to improve turbine performance. These concepts are typically designed to utilize residual steam velocity at the exit of a turbine stage. Several turbine concepts have been developed to accomplish this velocity utilization.

If multiple blade rows are applied, the turbine is said to be velocity compounded. This is sometimes called Curtis staging and a typical two-row Curtis stage consists of four rows of blades: a convergent-divergent nozzle, a rotor, a stator whose funtion is guidance and not change of pressure, and another rotor.

Analysis of the velocity compounded turbine indicates that the optimum speed ratio, ρ , (blade speed divided by steam jet velocity) is between 0.22 and 0.24 for two stages. This compares to a value of 0.45 for a single stage impulse turbine. Figure 4 is a comparison of the estimated efficiency of a two-stage, velocity compounded turbine compared to a single stage impulse turbine. As may be noted, at low speed ratios, the velocity compounded turbine offers a performance advantage over the single stage impulse turbine; however, the maximum efficiency at the optimum speed ratio is lower because of higher blading frictional losses. In general, it was found that, if near optimum speed ratios could be obtained for a given turbine stage, the impulse stage rather than the Curtis stage obtained the highest stage efficiency.

The primary area of application for a velocity compounded turbine stage is consequently one in which a high head drop per stage can be used to reduce the total number of stages in a multi-stage turbine that would otherwise require a large number of stages. Some penalty in performance must be tolerated, however, to allow a smaller overall turbine size and, therefore, lower cost.

4.2.2 Drag or Terry Turbines

Other single disc turbines such as drag or terry turbines, in which the steam is directed against the same turbine rotor a number of times, displayed results similar to those of the velocity compounded turbine. Maximum stage efficiencies between 40 and 50% were estimated for these turbine concepts at specific speeds less than 20.

The advantages of the drag or terry turbine are ruggedness and low cost. However, a substantial efficiency penalty is predicted as compared to a single axial flow stage. Because of this efficiency penalty, terry turbines do not appear to be well suited for use in solar-assisted cooling cycles.

4.3 LOW VOLUMETRIC FLOW TURBINE

The axial flow concept considered in this section was originally proposed by the Nuclear Power Field Office, R & T Department, Fort Belvoir, Virginia. Although this concept is in the conceptual phase and has not been fabricated or tested, a preliminary analysis (Ref. 4) and design were completed by Barber-Nichols. The LVFT is discussed in this section since it

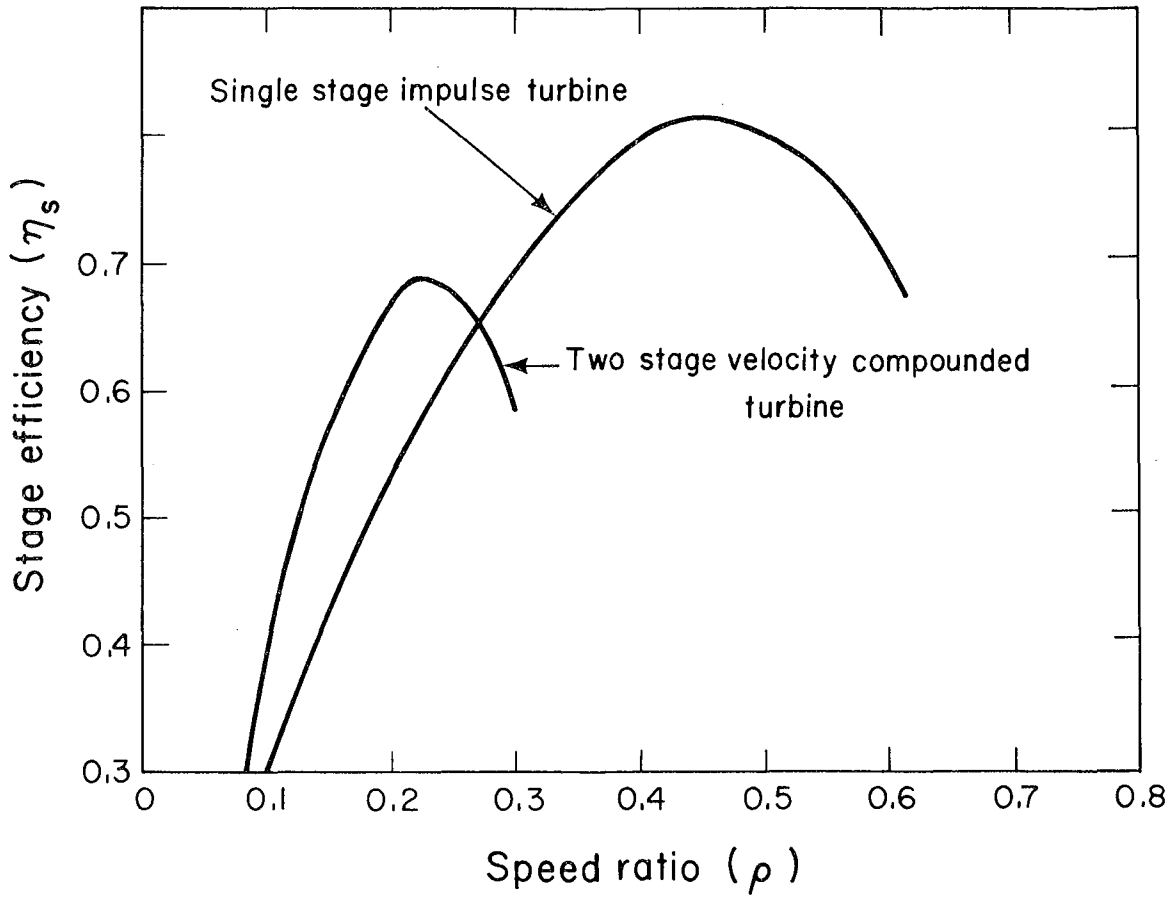

XBL 7711-11304

Fig. 4 Comparison of Efficiencies for Impulse and Velocity Compounded Turbine Stages

was conceived particularly for use in areas of low turbine specific speed. At levels of output power between 1 and 3 hp, and for the conditions of the present study, the values of specific speed calculated for the turbine are in a range where the LVFT can offer a performance advantage in a multi-stage configuration.

The following section discusses the concept and estimated performance.

4.3.1 Description

A schematic of this turbine concept is shown in Figure 5. Steam entering the turbine expends a portion of the available energy in nozzles arranged around the periphery of the stator. The steam, accelerated to wheel speed, enters a plenum in the turbine rotor. Nozzles spaced around the rotor then expand and direct steam opposite to the rotation of the turbine from which energy is extracted. As may be noted, this concept can result in a partial admission and partial emission turbine assembly. This allows optimally designed flow passages and high blading efficiency in cases of low turbine flow rates since not all the rotor periphery is filled with flow passages.

A key element in achieving high turbine efficiency is the performance of the close clearance seals. Because of the importance of these elements a follow-on program was conducted (Ref. 5) to fabricate and test seal segments in a simulated turbine design. Design criteria for these seals was verified in the test program and primary seal leakage comparisons between predicted and actual data were found to be accurate. Because of the conceptual nature of this concept, some development effort is anticipated to obtain high efficiency and reliable performance.

4.3.2 Estimated Performance

The method of calculation used to predict overall turbine efficiency was similar to that presented in section 4.1 for the conventional axial flow stages. Using calculated values of stage specific speed, stage efficiency was estimated from Figure 6. This diagram was constructed based on previous analysis and includes blading efficiency, windage losses, and seal leakage calculated as a function of turbine specific speed. Additional losses associated with Reynolds number, Mach number, and non-optimum U/C_o were estimated and deducted from the diagram efficiency to obtain an overall stage efficiency.

Calculated performance for a four-stage LVFT turbine at 1 hp and 75,000 rpm is summarized in Table III. These efficiencies were combined to yield an overall efficiency of 71% which is substantially greater than calculated for conventional axial flow stages at the same speed and power level. Additional study is needed to weigh the potential performance advantage of the LVFT applied in small solar-assisted cooling cycles against the development effort required to utilize this turbine concept.

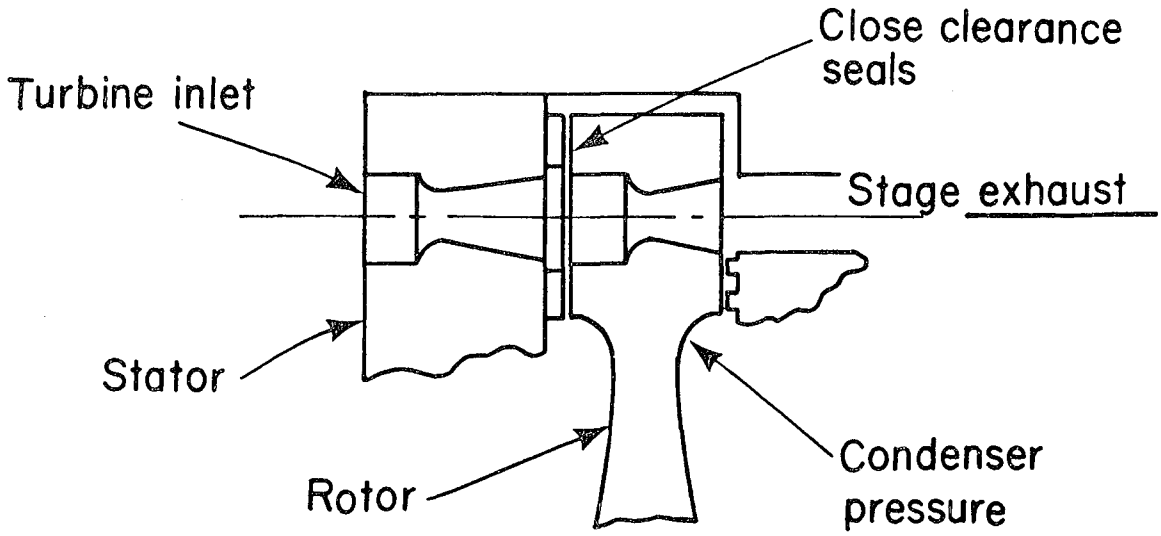

XBL7711-2197

Fig. 5 Low Volumetric Flow Turbine Stage

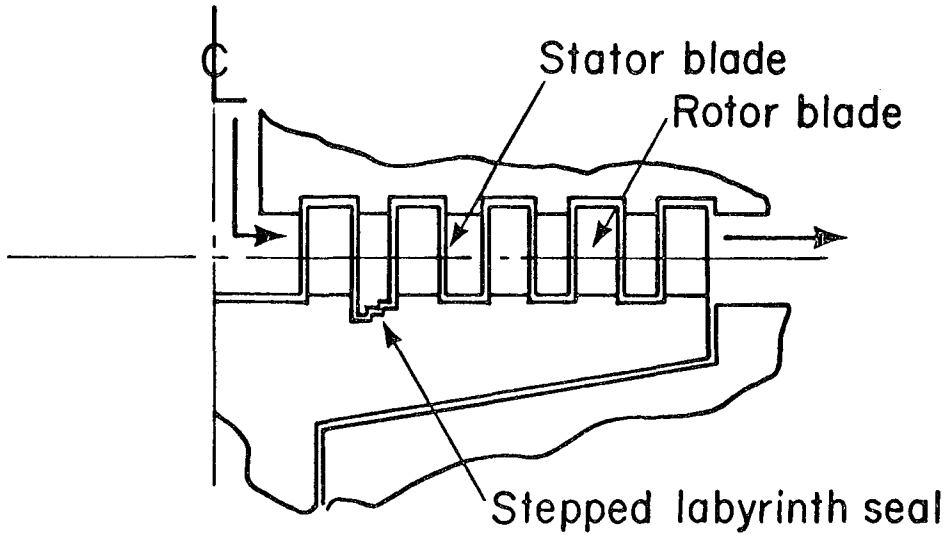

XBL7711-2196

Fig. 7 Multi-Stage Radial Outflow Turbine

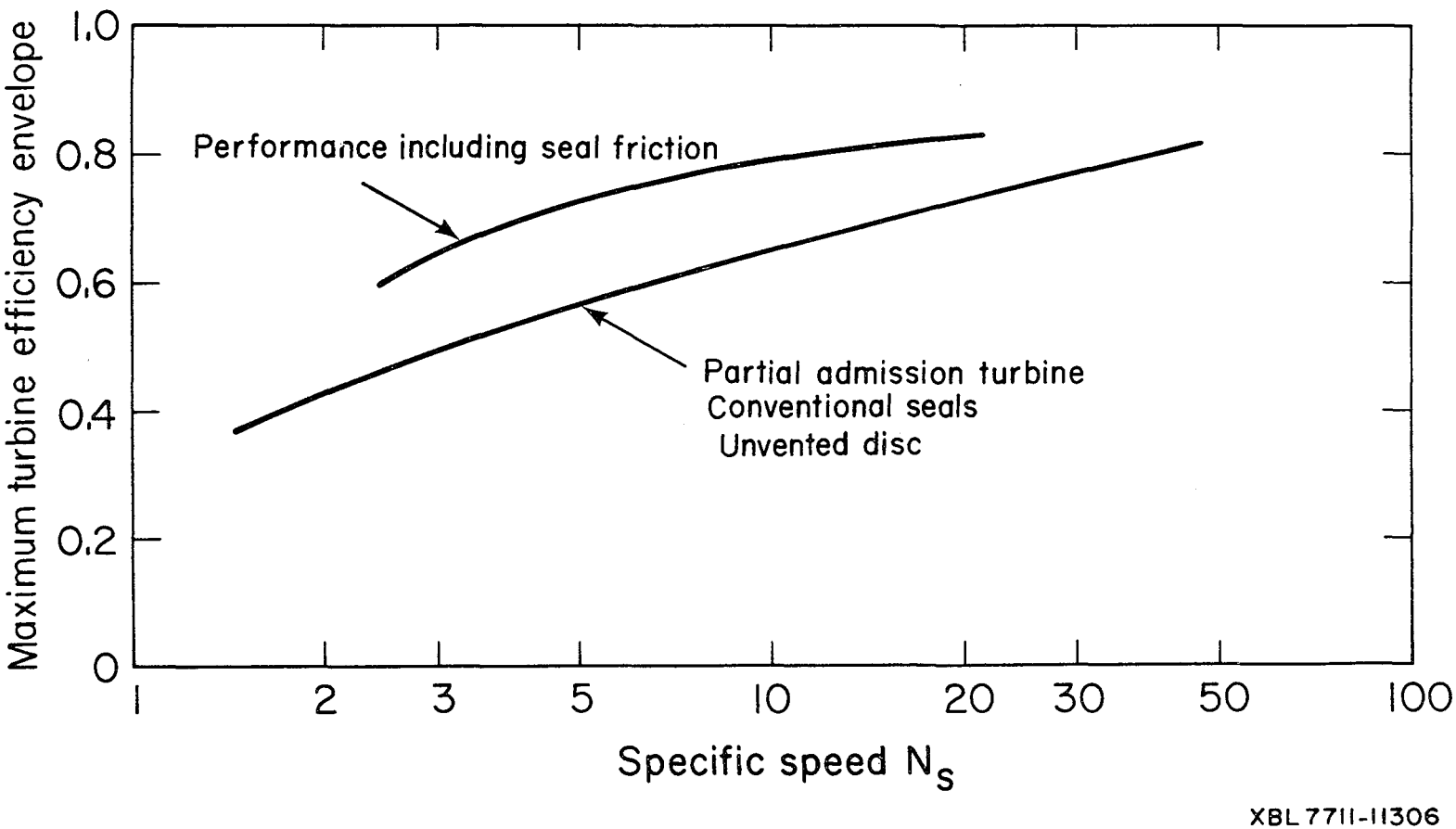

Fig. 6 Turbine Performance 3-Seals Vented Disc

0 0 0 3 4 9 0 1 2 4 8

TABLE III

SUMMARY OF LVFT PERFORMANCE

Stage	Available Energy, Btu/lb	Diameter, in.	N_s	Corrected Stage Efficiency
1	123.3	3.94	3.0	58%
2	123.3	4.58	4.3	67%
3	123.3	4.58	6.5	65%
4	136.9	4.58	10.9	62%

5.0 RADIAL OUTFLOW SINGLE DISC TURBINE

5.1 TURBINE DESCRIPTION

The turbine evaluated in this section is similar in design to the Ljungstrom turbine which, although uncommon in the U. S., has received considerable acceptance in Europe. The normal Ljungstrom turbine has no stators, both sets of blades comprising a stage having opposite rotation. However, the turbine evaluated and discussed in this report is a single disc turbine with the second rotor fixed to form a stator. This turbine is shown schematically in Figure 7.

Steam flows from the center of the disc outward, so that as the steam density decreases a greater flow area is encountered because of the change in radius. In this way the change in blade height from the first to the last stages is minimized. The blade rows also must be properly designed so that the energy in the form of steam velocity leaving a rotating blade row is available to the following stator row. The method of analysis and predicted performance are presented in the following sections.

5.2 PERFORMANCE EVALUATION

The cycle evaluated was again the solar-assisted Rankine cycle which was evaluated with the conventional axial flow impulse turbine. The radial outflow turbine was evaluated at 1, 5, and 10 hp and 50,000 rpm in a five-stage and a six-stage configuration.

5.2.1 Assumptions

A number of assumptions were made to facilitate evaluation of the radial outflow turbine, minimize leakage, and estimate a maximum overall turbine efficiency. A condition line describing the head drop per stage was evaluated. Equal head drop per stage such as was used with the axial flow configuration is not optimum for the radial flow turbine. Because of the changing radius of the turbine stages, the optimum conditions line involves a trade-off between stage velocity ratio and leakage losses. Several condition lines were evaluated for the turbine and the values presented in this section resulted in the highest overall turbine efficiency.

Two assumptions, which ease calculation of hydraulic efficiencies for each stage, are that the diameter and, therefore, rotor speed, which are increasing across the rotor blade tips, are taken as an average diameter and an average rotor tip speed at the center of the rotor chord.

A further assumption that eased the calculation of rotor inlet and exit relative velocities was that the rotor blades were symmetrical and that the inlet and exit blade angles were therefore equal.

The final assumption was that velocity utilization in succeeding stages from fluid exiting preceeding stages was 42%. This assumption corresponds to well-designed blade elements with large angular deflection of the steam. This resulted in an increase in total enthalpy drop across stages 2 through 5 or 6.

5.2.2 Method of Evaluation

To evaluate the performance of the radial outflow turbine a rotor diameter and a maximum angular velocity were first selected. The diameter was selected based on tip speed of the last stage rotor. The tip speed was limited to 1500 ft/sec based on stress considerations. Diameters were calculated based on rotor speeds of 25,000 to 100,000 rpm. A disc friction or windage loss was then calculated from the expression

$$HP_d = \frac{Kw\ \rho_e D^2 U^2}{g\ (550)}$$

where	Kw	=	a constant equal to 0.001
	ρ_e	=	exit fluid density, typically 0.003 lbm/ft^3
	D	=	rotor tip diameter
	U	=	rotor tip velocity in ft/sec
	g	=	32.2 ft/sec^2

Table IV shows values of windage horsepower loss as a function of rpm for a constant tip speed and 1500 ft/sec. Considering a minimum horsepower output of 1 hp, windage loss alone is seen to be 75-5% of the output power. High rotational speeds and small turbine diameters are therefore required to achieve high efficiencies. Sufficient diameter is necessary, however, in order to utilize 5 or 6 stages while maintaining reasonable blade chords of 0.2 inch or greater. It should be noted that maximum blade speeds less than 1500 ft/sec consistently result in lower overall turbine efficiencies. Lower blade speeds require substantially more pressure compounded stages (8-10) to achieve optimum efficiency and the correspondingly larger wheel diameters result in increased parasitic loss as above.

Based on the above analysis, a 6 inch diameter rotor disc was chosen and, to keep the tip speed below 1500 ft/sec, a rotational speed of 50,000 rpm was chosen. A five-stage and a six-stage turbine were analyzed. The average diameter of each ring of rotor blades was calculated using the center of the chord of each stage blade ring as the average diameter for each stage. The average blade tip velocity was then calculated. A head drop across each stage was chosen based on considerations discussed in section 5.1.2.1, the isentropic head drop from 1100°F and 89.7 psia to 1.7 psia, and reheat based on the equations

$$R = 1 + (R_\infty - 1)\left(1 - \frac{1}{n}\right)\left(\frac{1-\eta_s}{0.2}\right)$$

and

$$\Delta H' = R\ \Delta H'_{id}$$

The total head drop across the first stage was set equal to the selected isentropic head drop since there was no velocity utilization from preceeding stages.

A value of U/C_o was then calculated from the equation

TABLE IV

WINDAGE HORSEPOWER LOSS FOR RADIAL TURBINES

N	Diameter (max.)	HP_d
25,000	13.75	0.751
50,000	6.88	0.188
75,000	4.58	0.083
100,000	3.44	0.047

$$U/C_o = \frac{U_{ave}}{\sqrt{2gJ\Delta Hs'_{tot}}}$$

where U_{ave} = average velocity of the rotor

$\Delta Hs'_{tot}$ = total head drop across the stage

A nozzle velocity coefficient (ψ_n) of 0.92, a rotor velocity coefficient (ψ_r) of 0.75, and a nozzle angle of 16° were chosen based on well-designed blade elements. The hydraulic efficiency of each stage was then determined from the equation

$$\eta_H = 2\frac{U}{C_o}(\psi_n \cos\alpha - U/C_o)(1 + \psi_r),$$ which is derived

from the equation

$$\eta_H = \frac{2\,U_1\,(Cu_1 + Cu_2)}{Co^2}$$

where Co = isentropic spouting velocity

U_1 = rotor blade velocity

Cu_1 = tangential component of inlet fluid velocity

Cu_2 = tangential component of exit fluid velocity

The increase in head and the total head for the next stage were then calculated from the expressions

$$\Delta Hs_{tot} = \Delta Hs + 0.42\,C_3^2/2gJ$$

Where C_3 is the absolute exit fluid velocity of the stage being examined,

$$C_3 = Cu_3^2 + Ca_3^2$$

Where u_3 is the tangential component and a_3 is the radial component of fluid exit velocity,

$$Cu_3 = \psi_n Co \cos\alpha - \frac{\eta_H\, gJ\Delta Hs_{tot}}{U_{ave}},$$

and $$Ca_3 = \psi_n \psi_r Co \sin\alpha$$

The actual head drop ΔHa was then calculated from

$$\Delta Ha = \eta_H \Delta Hs_{tot}$$

The above procedure was repeated for the remaining stages using the ΔHs_{tot} instead of ΔHs_{isen} and insuring that the fluid in the final stage expanded to 1.7 psia.

The overall hydraulic efficiency was then calculated from the expression

$$\eta_{H_{overall}} = \frac{\sum \Delta H_a}{\Delta H'_{id}}$$

5.2.3 Determination of Losses

The losses that have the greatest effect on the radial outflow turbine are disc friction or windage loss and leakage loss. The windage loss was evaluated using the equation

$$HP_d = Kw \frac{\rho_e}{g} \frac{D^2U^3}{550}$$

where	Kw	=	a constant equal to 0.001
	ρ_e	=	exit density of the fluid leaving the last stage and is typically 0.003 lbm/ft^3
	D	=	rotor diameter
	U	=	rotor tip velocity
	g	=	32.2 ft/sec^2

The leakage loss was claculated using the equation

$$HP_l = GH\,(778)/\eta_H(550)$$

where	G	=	leakage in lbm/sec
	H	=	total enthalpy drop across a stage
	η_H	=	hydraulic efficiency of the stage

To determine the leakage loss, the chord length of a turbine blade was first calculated from the equation

$$\text{Chord Length} = \frac{\frac{(D_t - D_s)}{2} - (2n - 1)(C_l)}{2n}$$

where	D_t	=	rotor diameter
	D_s	=	shaft diameter
	n	=	number of stages
	C_l	=	clearance between rotor and stator blade rings

Referring to Figure 9 of Egli (Ref. 6) for a staggered labyrinth, values of seal thickness Δ, seal clearance δ, and pitch s , were chosen based on the blade chord determined above.

The labyrinth pressure ratio across each seal was calculated assuming that the pressure drop across each labyrinth was equal to the stage pressure ratio.

The cross sectional leakage area of each seal was calculated from the

equation

$$A = \pi D \delta$$

where D = average diameter of each stage
δ = seal clearance

The leakage in lbm/sec was then calculated from the equation

$$G = A \alpha \phi \gamma \left(g \frac{Po}{v_o}\right)^{1/2}$$

where A = seal leakage area
α = flow coefficient for labyrinths with sharp edged strips and was determined from Figure 18 of Egli
ϕ = leakage function determined from Figure 7 of Egli
γ = a correction factor that corrects for non-ideal labyrinths and was set equal to one.
Po = absolute pressure before the labyrinth
v_o = specific volume before the labyrinth

With values of G, H, and η_H known for each stage, a horsepower loss due to leakage was then calculated for each stage using the equation for HP_1.

5.2.4 Overall Turbine Performance

To determine the overall efficiency of the turbine, an equation for overall efficiency based on the expression

$$\text{Overall Efficiency} = \frac{\text{Actual Work}}{\text{Ideal Work}}$$

was derived. The derivation resulted in the equation

$$\eta_{overall} = \frac{\eta_{H_{overall}} (DHP)}{(DHP + \sum HP_1 - HPd)}$$

where $\eta_{H_{overall}}$ = the overall hydraulic efficiency determined from

$$\eta_{H_{overall}} = \frac{\sum \Delta Ha}{\Delta H'_{id}}$$

DHP = Desired horsepower output
$\sum HP_1$ = summation of leakage losses in each stage
HPd = windage loss

5.3 TURBINE PERFORMANCE EVALUATION

The results of the turbine performance evaluation are presented in Table V. Since the axial turbo-expander performance was not evaluated at precisely the conditions listed in Table V, an approximate comparison can be presented. Comparing the six-stage, 1 hp, 50,000 rpm radial outflow turbine to the 1 hp, axial turbine with one stage at 50,000 rpm and six stages at 90,000 rpm, the overall efficiencies of the axial turbines are 38.3% and 54.9% respectively, compared to 23.8% for the radial outflow turbine. Based on these data and data for other combinations of stages, horsepower output and rpm, the efficiency of a six-stage, 1 hp, 50,000 rpm, axial turbine would be approximately 52%, or nearly twice that of a radial outflow turbine operating under the same conditions.

Basic problems exist with the single disc radial outflow turbine that limit the achievable efficiency of this concept. First, geometric considerations along with reasonable blade chords limit the number of stages that can be incorporated in the turbine design. Secondly, high windage loss compared to the output power is the result of selecting adequate turbine rotor diameter to achieve reasonable stage numbers. These considerations are apparent in the first stages where low stage velocity ratios result in low stage efficiency.

Appendix II presents the detailed calculations for the two radial outflow turbines examined.

6.0 CONCLUSIONS

1. High efficiency (greater than 70%) centrifugal compressors can be utilized over the range of conditions selected in this study. At very low capacities, approximately one ton AC, a maximum compressor efficiency of 65% was estimated. This causes a slight reduction in COP_{VC} of from 4 to 3.7. Matching characteristics between the vapor compressor and the turbine indicate optimum rotational speeds between 50-80,000 rpm for the range of power examined.

2. Multi-stage axial flow turbines can be used for the selected cycle conditions to achieve efficiency levels greater than 80%. Regardless of the number of stages used, the minimum power level for which 80% efficiency can be achieved is approximately 20 hp.

3. Multi-row, single disc turbines can be used to reduce expander cost for certain applications; however, in each case examined, a performance penalty was incurred by using a single disc rotor as compared to conventional axial flow stages.

4. Advanced concept, low specific speed turbines can be used to improve turbine efficiency at power levels below 20 hp. Development risk for these turbines must be considered high.

TABLE V

SUMMARY OF RADIAL OUTFLOW TURBINE EFFICIENCY

Stages	1		5		10	
	rpm	η_t	rpm	η_t	rpm	η_t
5	50 K	21.9%	50 K	49.6%	50 K	58.9%
6	50 K	23.8%	50 K	50.5%	50 K	58.7%

5. Based on the overall performance of the turbomachinery, the solar-assisted Rankine cycle appears best suited for cooling loads between 15 and 75 tons. Additional study would be needed to evaluate comparative costs and performance between conventional Rankine cycle, absorption machinery, and the solar-assisted approach at these higher cooling capacities.

6. An improved estimate of turbomachinery performance at one to three tons of air conditioning, and for the cycle conditions specified in the study may be summarized:

a)	Vapor compressor efficiency	=	65%
b)	COP vapor cycle	=	3.7
c)	Turbo-expander efficiency	=	70%

With these values of efficiency, an improved evaluation of the solar-assisted Rankine cycle could be completed.

7.0 REFERENCES

1. Curran, H. M. "Assessment of Solar Powered Cooling of Buildings," NSF-RA-N-75-02, April, 1975.

2. Balje, O. E. and Binsley, R. L. "Axial Turbine Performance Evaluation Part B - Optimization With and Without Constraints," Journal of Engineering for Power, October, 1968.

3. Church, Edwin F., Jr. S.B., S.M. Steam Turbines. Second Edition, Tenth Impression, McGraw-Hill Book Co. Inc., New York, NY, 1935.

4. Nichols, K. E. "Low Volumetric Flow Turbine Performance Prediction and Analysis Final Report," Barber-Nichols Engr. Co. report, March, 1968.

5. Welz, H. C. "Final Report on the Low Volumetric Flow Turbine Design," Barber-Nichols Engr. Co. report, February, 1971.

6. Egli, Adolf "The Leakage of Steam Through Labyrinth Seals," Transactions of the ASME, Fuel and Steam Power, FSP-57-5.

APPENDIX

I Detailed Calculations for Six-Stage, 90,000 rpm, Axial Turbine at 1 and 25 horsepower.

II Detailed Calculations for Five and Six-Stage, 50,000 rpm, Radial Outflow Turbine at 1, 5, and 10 horsepower.

III Coefficient of Performance of Rankine System.

IV Vapor Compressor Operating Characteristics.

Appendix I

SIX STAGE 90,000 RPM TURBINE
PERFORMANCE @ 1 AND 25 hp

Speed	: 90,000 rpm	P_1 =	89.64 psia	T_{11}	=	T_{12}	=	320°F
Stages	: 6	T_1 =	1100°F	T_8	=	T_9	=	120°F
hp	: 1 and 25	P_7 =	1.7 psia					

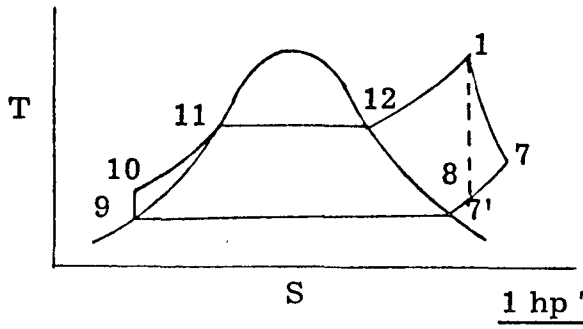

From Mollier Diagram

T_7' = 170°F
H_1 = 1584 Btu/lbm
H_7' = 1136 Btu/lbm
H'_{id} = 448 Btu/lbm

1 hp Turbine

Assume a first stage and overall efficiency of 60%.

$R = 1 + (R_\infty - 1)(1 - 1/n)[(1 - \eta e)/0.2] = 1 + (1.09 - 1)(1 - 1/6)[(1-0.6)/0.2] = 1.15$

$H'/\text{stage} = (R\Delta H_{id}/n) = [1.15(448)/6] = 85.862$ Btu/lbm

$\dot{w} = [HP(550)/\eta e\Delta H'_{id}(778)] = [1(550)/0.6(448)(778)] = 0.0026$ lb/sec

from the Mollier Diagram with an isentropic drop in H of 85.862; P_2 = 52 psia

$H_{2e} = H_1 - \eta e\Delta H' = 1584-0.6(85.862) = 1532.48$

$Qe = \nu e\dot{w} = 16.62(0.0026) = 0.0433\ ft^3/sec$

$Ns = N\sqrt{Qe}/(\Delta H'id_s J)^{3/4} = 90,000(0.0433)^{1/2}/[(85.862)(778)]^{3/4} = 4.505$

Assume U/Co = 0.375 $\qquad \eta_D = 0.55$

$D_s = (U/Co)(154)/Ns = 0.375(154)/4.505 = 12.82$

$U = (U/Co)\sqrt{2gJ\Delta H'id_s} = 0.375\ (2)(32.2)(778)(85.862)$
$= 0.375(2074.14) = 777.80$ ft/sec

$\therefore \eta/\eta_D(U/Co) = 1$

$Dia = U(720)/\pi N = 777.80(720)/\pi(90,000) = 1.981$ inches

$Re^* = U/12\,(Dia\,\rho/\mu g) = 777.80(1.981)/12(16.62)(6.3 \times 10^{-7})(32.2) = 3.81 \times 10^5$

$\therefore \eta/\eta_D(Re^*) = 0.89$

from Mach Tables @ $\gamma = 1.3$ and $P_R = P_2/P_1 = 52/89.64 = 0.5801$; $M' = 0.945$

$AMR = 0.94[1-(U/Co)]\,M' = 0.94\,(1-0.375)(0.945) = 0.555$

$\therefore\ \eta/\eta_D\,(AMR) = 1$

$h/D = 0.018$

$h = 0.018\,(1.981) = 0.0357$ inches

$\eta s = \eta D[\eta/\eta D(U/Co)][\eta/\eta D(Re^*)][\eta/\eta D(AMR)]$

$= 0.55(1)(0.89)(1) = 0.4895$

$Hea = H_1 - \eta_s \Delta H' = 1584 - 0.4895(85.862) = 1541.97$

$\Delta Ha = \eta_s \Delta H' = 0.4895(85.862) = 42.029$

Assume a 2nd stage efficiency of 50%

$H_{3e} = 1541.97 - 0.5(85.862) = 1499.04$

from Mollier Diagram with an isentropic drop in H of 85.862 ; $P_3 = 29.5$ psia

$Qe = \nu e \dot{w} = 28.06(0.0026) = 0.0730\ ft^3/sec$

$N_s = 90(0.270)/4.155 = 5.851$

$\eta_D = 0.59$ Assume a $U/Co = 0.396$

$D_s = 0/396(154)/5.851 = 10.423$

$U = 0.396(2074.14) = 821.36$ ft/sec

$\therefore\ \eta/\eta_D\,(U/Co) = 1$

$Dia = 821.36(720)/\pi(90,000) = 2.09$ inches

$Re^* = 821.36(2.09)/\ 12(28.06)(5.9 \times 10^{-7})(32.2) = 2.68 \times 10^5$

$\therefore\ \eta/\eta_D(Re^*) = 0.85$

from Mach Tables @ $\gamma = 1.3$ and $P_R = P_3/P_2 = 29.5/52 = 0.5673$; $M' = 0.965$

$AMR = 0.94\,(1-0.396)(0.965) = 0.548$

$\therefore\ \eta/\eta_D(AMR) = 1$

$h/D = 0.02$

$h = 0.02\ (2.09) = 0.0418$ inches

% leakage = $Cl/h\ (100) = 0.005/0.0418\ (100) = 11.96\%$

$\eta_s = 0.59(1)(0.85)(1)(1 - 0.1196) = 0.4415$

$H_{ea} = H_2 - (\eta_s/1 - L)\Delta H' = 1541.97 - (0.4415/1 - 0.1196)(85.862) = 1498.89$

$\Delta Ha = \eta_s \Delta H' = 0.4415\ (85.862) = 37.91$

Assume a 3rd stage efficiency of 50%

$He_4 = 1498.89 - 0.5(85.862) = 1455.63$

from Mollier Diagram with isentropic drop in H of 85.862 ; $P_4 = 16.2$ psia

$Qe = v_e \dot{w} = 48.56\ (0.0026) = 0.126\ ft^3/sec$

$Ns = 90(0.335)/\ 4.155 = 7.696$

$\eta_D = 0.63$ Assume $U/Co = 0.427$

$Ds = 0.427(154)/7.696 = 8.544$

$U = 0.427(2074.14) = 885.66$ ft/sec

$Dia = 885.66(720)/\pi(90,000) = 2.255$ inches

$Re^* = 885.66(2.255)/\ 12(48.56)(5.5 \times 10^{-7})(32.2) = 1.936 \times 10^5$

$\therefore \eta/\eta_D\ (Re^*) = 0.84$

from Mach Tables @ $\gamma = 1.3$ and $P_R = P_4/P_3 = 16.2/29.5 = 0.5492$; $M' = 0.994$

$AMR = 0.94(1 - 0.427)(0.994) = 0.535$

$\therefore \eta/\eta_D(AMR) = 1$

$h/D = 0.022$

$h = 0.022(2.255) = 0.0496$ inches

% leakage = $0.005/0.0496\ (100) = 10.08\%$

$\eta_s = 0.63(1)(0.84)(1)(0.899) = 0.4759$

$He_a = 1498.89 - (0.4759/0.899)\ 85.862 = 1453.44$

$\Delta Ha = 0.4759(85.962) = 40.858$

Assume a 4th stage efficiency of 50%

$He_5 = 1453.44 - 0.5(85.862) = 1410.51$

from Mollier Diagram with isentropic drop in H of 85.862 ; $P_5 = 8.5$ psia

$Qe = \nu ew = 84.97(0.0026) = 0.221\ ft^3/sec$

$Ns = 90(0.470)/4.155 = 10.181$

$Ds = 5.70 \qquad \eta_D = 0.665$

$U/Co = NsDs/154 = 10.181(5.70)/154 = 0.377$

$U = 0.377(2074.14) = 781.95$ ft/sec

$\therefore \eta/\eta_D(U/Co) = 1$

$Dia = 781.95(720)/\pi(90,000) = 1.99$ inches

$Re^* = 781.95(1.99)/12(84.97)(5.1 \times 10^{-7})(32.2) = 0.929 \times 10^5$

$\therefore \eta/\eta_D\ (Re^*) = 0.725$

from Mach Tables @ $\gamma = 1.3$ and $P_R = P_5/P_4 = 8.5/16.2 = 0.52469$; $M' = 1.034$

$AMR = 0.94(1 - 0.377)(1.034) = 0.606$

$\therefore \eta/\eta_D\ (AMR) = 1$

$h/D = 0.028 \qquad h = 0.028(1.99) = 0.0557$ inches

% leakage = 0.005/0.0557(100) = 8.98%

$\eta_s = 0.665(1)(0.725)(1)(0.910) = 0.4388$

$He_a = 1453.44 - (0.4388/0.910)\ 85.862 = 1412.03$

$\Delta Ha = 0.4388(85.862) = 37.676$

Assume a 5th stage efficiency of 45%

$He_6 = 1412.03 - 0.45(85.862) = 1373.39$

from Mollier Diagram for an isentropic drop in H of 85.862 ; $P_6 = 4.25$ psia

$Qe = \nu e\dot{w} = 161.21(0.0026) = 0.419\ ft^3/sec$

$Ns = 90(0.647)/4.155 = 14.023$

$Ds = 4.20$ $\eta D = 0.70$

$U/Co = 14.023(4.20)/154 = 0.382$

$U = 0.382(2074.14) = 793.27$ ft/sec

$\therefore \eta/\eta_D (U/Co) = 1$

$Dia = 793.27(720)/\pi(90,000) = 2.02$ inches

$Re^* = 793.27(2.02)/12(161.21)(4.7 \times 10^{-7})(32.2) = 0.547 \times 10^5$

$\therefore \eta/\eta_D (Re^*) = 0.68$

from Mach Tables @ $\gamma = 1.3$ and $P_R = P_6/P_5 = 4.25/8.5 = 0.5000$; $M' = 1.075$

$AMR = 0.94(1 - 0.382)(1.075) = 0.624$

$\therefore \eta/\eta_D (AMR) = 1$

$h/D = 0.035$ $h = 0.035(2.02) = 0.0707$ inches

% leakage = 0.005/0.0707 (100) = 7.072%

$\eta_s = 0.70(1)(0.68)(1)(0.929) = 0.4423$

$He_a = 1412.03 - (0.4423/0.929)\ 85.862 = 1371.15$

$\Delta Ha = 0.4423\ (85.862) = 37.98$

Assume a 6th stage efficiency of 45%

from Mollier Diagram with isentropic pressure drop to $P_7 = 1.7$ psia

$\Delta H' = 1371.154 - 1270.00 = 101.154$

$He_6 = 1371.154 - 0.45\ (101.154) = 1325.635$

$Qe = \nu e \dot{w} = 363.57(0.0026) = 0.945\ ft^3/sec$

$Ns = 90(0.972)/4.70 = 18.613$

$Ds = 3.40$ $\eta D = 0.727$

$U/Co = 18.613(3.40)/154 = 0.411$

$U = 0.411(2251.253) = 925.265$ ft/sec

$\therefore \eta/\eta D\ (U/Co) = 1$

Dia = 925.265(720)/π(90,000) = 2.356 inches

Re* = 925.265(2.356)/ 12(363.57)(4.3 x 10^{-7})(32.2) = 0.361 x 10^5

$\therefore \eta/\eta D(Re^*) = 0.70$

from Mach Tables @ γ= 1.3 and $P_R = P_7/P_6$ = 1.7/4.25 = 0.4000 ; M' = 1.250

AMR = 0.94(1 - 0.411)(1.250) = 0.692

$\therefore \eta/\eta_D$ (AMR) = 1

h/D = 0.055 h = 0.055(2.356) = 0.1296 inches

% leakage = 0.005/0.1296 (100) = 3.858%

ηs = 0.727(1)(0.70)(1)(0.961) = 0.4893

Hea = 1371.154 - (0.4893/0.961) 101.154 = 1319.651

ΔHa = 0.4893(101.154) = 49.491

η overall = (49.491 + 37.980 + 37.676 + 40.858 + 37.908 + 42.029)/ 448

= 245.342/448 = 0.5490 = 54.90%

---

25 hp Turbine

Assume a 1st stage and an overall efficiency of 70%

R = 1 + (1.09 - 1)[1 - (1/6)] [(1-0.7)/0.2] = 1.112

ΔH'/stage = 1.112(448)/6 = 83.029 Btu/lbm

$\dot{w}$ = 25(550)/ 0.7(448) (778) = 0.0564 lb/sec

H_{2e} = 1584 - 0.70(83.029) = 1525.88

from Mollier Diagram with isentropic drop in H of 83,029 Btu/lbm ; P_2 = 53 psia

Qe = $v_e\dot{w}$ = 16.25(0.0564) = 0.9165 ft^3/sec

Ns = 90(0.957)/4.05 = 21.267

Ds = 3.10 ηD = 0.740

$U/Co = 21.267(3.10)/154 = 0.428$

$U = 0.428\sqrt{2(32.2)(778)(83.029)} = 0.428(2039.6) = 873.14$ ft/sec

$\therefore \eta/\eta_D(U/Co) = 1$

$Dia = 873.14(720)/\pi(90,000) = 2.22$ inches

$Re^* = 873.14(2.22)/12(16.25)(6.2 \times 10^{-7})(32.2) = 4.99 \times 10^5$

$\therefore \eta/\eta_D(Re^*) = 0.94$

from Mach Tables @ $\gamma = 1.3$ and $P_R = P_2/P_1 = 53/89.64 = 0.5913$; $M' = 0.927$

$AMR = 0.94(1 - 0.428)(0.927) = 0.498$

$\therefore \eta/\eta_D(AMR) = 1$

$h/D = 0.060$ $\qquad h = 0.060(2.22) = 0.133$ inches

$\eta s = 0.740(1)(0.94)(1) = .6956$

$He_a = 1584 - 0.6956(83.029) = 1526.245$

$\Delta Ha = 0.6956(83.029) = 57.755$

Assume a 2nd stage efficiency of 70%

$H_{3e} = 1526.245 - 0.70(83.029) = 1468.125$

from Mollier Diagram with isentropic drop in H of 83.029 Btu/lbm ; $P_3 = 31$ psia

$Qe = \nu e\dot{w} = 25.5(0.0564) = 1.438$ ft^3/sec

$Ns = 90(1.199)/4.05 = 26.644$

$Ds = 2.65$ $\qquad \eta_D = 0.758$

$U/Co = 26.644(2.65)/154 = 0.458$

$U = 0.458(2039.6) = 935.14$ ft/sec

$\therefore \eta/\eta_D(U/Co) = 1$

$Dia = 935.14(720)/\pi(90,000) = 2.381$ inches

$Re^* = 935.14(2.381)/12(25.5)(5.7 \times 10^{-7})(32.2) = 3.96 \times 10^5$

$\therefore \eta/\eta_D(Re^*) = 0.94$

from Mach Tables @ $\gamma = 1.3$ and $P_R = P_3/P_2 = 31/53 = 0.5849$; $M' = 0.938$

$AMR = 0.94(1 - 0.458)(0.938) = 0.4779$

$\therefore \eta/\eta_D(AMR) = 1$

$h/D = 0.065$ $\qquad$ $h = 0.065(2.381) = 0.1548$ inches

% leakage = 0.005/0.1548 (100) = 3.23%

$\eta s = 0.758(1)(0.94)(1)(0.968) = 0.6895$

$Hea = 1526.245 - (0.6895/0.968)(83.029) = 1467.104$

$\Delta Ha = 0.6895(83.029) = 57.249$

Assume a 3rd stage efficiency of 72%

$He_4 = 1467.104 - 0.72(83.029) = 1407.323$

from Mollier Diagram with an isentropic drop in H of 83.029 Btu/lbm ; $P_4 = 17$ psia

$Qe = \nu e \dot{w} = 42.24(0.0564) = 2.382\ ft^3/sec$

$Ns = 90(1.543)/4.05 = 34.298$

$Ds = 2.25$ $\qquad$ $\eta_D = 0.780$

$U/Co = 34.298(2.25)/154 = 0.5011$

$U = 0.5011(2039.6) = 1022.05$ ft/sec

$\therefore \eta/\eta_D(U/Co) = 1$

$Dia = 1022.05(720)/\pi(90,000) = 2.603$ inches

$Re^* = 1022.05(2.603)/12(42.24)(5.1 \times 10^{-7})(32.2) = 3.20 \times 10^5$

$\therefore \eta/\eta_D(Re^*) = 0.95$

from Mach Tables @ $\gamma = 1.3$ and $P_R = P_4/P_3 = 17/31 = 0.5484$; $M' = 0.996$

$AMR = 0.94(1 - 0.5011)(0.996) = 0.4671$

$\therefore \eta/\eta_D(AMR) = 1$

$h/D = 0.067$ $\qquad$ $h = 0.067(2.603) = 0.1744$ inches

% leakage = 0.005/0.1744(100) = 2.87%

ηs = 0.780(1)(0.95)(1)(0.971) = 0.7198

Hea = 1467.104 - (0.7198/0.971)(83.029) = 1405.55

ΔHa = 0.7198(83.029) = 59.761

Assume a 4th stage efficiency of 73%

He_5 = 1405.55 - 0.73(83.029) = 1344.939

from Mollier Diagram with isentropic drop in H of 83.029 Btu/lbm ; P_5 = 8.6 psia

Qe = $\nu e \dot{w}$ = 75.51(0.0564) = 4.259 ft^3/sec

Ns = 90(2.06)/4.05 = 45.862

Ds = 1.82 ηD = 0.800

U/Co = 45.862(1.82)/ 154 = 0.542

U = 0.542(2039.6) = 1105.47 ft/sec

$\therefore \eta/\eta_D$(U/Co) = 1

Dia = 1105.47(720)/π(90,000) = 2.815 inches

Re* = 1105.47(2.815)/ 12(75.50)(4.5 x 10^{-7})(32.2) = 2.37 x 10^5

$\therefore \eta/\eta_D$(Re*) = 0.96

from Mach Tables @ γ= 1.3 and $P_R = P_5/P_4$ = 8.6/17 = 0.5059 ; M' = 1.066

AMR = 0.94(1 - 0.542)(1.066) = 0.459

$\therefore \eta/\eta_D$(AMR) = 1

h/D = 0.060 h = 0.060(2.815) = 0.1689 inches

% leakage = 0.005/0.1689 (100) = 2.96%

ηs = 0.80(1)(0.96)(1)(0.971) = 0.7461

Hea = 1405.55 - (0.7461/0.971)(83.029) = 1341.752

ΔHa = 0.7461(83.029) = 61.945

Assume a 5th stage efficiency of 76%

$He_6 = 1341.752 - 0.76(83.029) = 1278.65$

from Mollier Di agram with an isentropic drop in H of 83.029 Btu/lbm ; $P_6 = 4$ psia

$Qe = \nu \dot{e}w = 139.80(0.0564) = 7.884\ ft^3/sec$

$Ns = 90(2.81)/4.05 = 62.40$

$Ds = 1.50$ $\qquad \eta_D = 0.825$

$U/Co = 62.40(1.50)/154 = 0.608$

$U = 0.608(2039.6) = 1239.64$ ft/sec

$Dia = 1239.64(720)/\pi(90,000) = 3.16$ inches

$Re^* = 1239.64(3.16)/12(139.80)(3.9 \times 10^{-7})(32.2) = 1.91 \times 10^5$

$\therefore \eta/\eta_D(Re^*) = 0.94$

from Mach Tables @ $\gamma = 1.3$ and $P_R = P_6/P_5 = 4.0/8.6 = 0.4651$; $M' = 1.135$

$AMR = 0.94(1 - 0.608)(1.135) = 0.418$

$\therefore \eta/\eta_D(AMR) = 1$

$h/D = 0.080$ $\qquad h = 0.080(3.16) = 0.253$ inches

% leakage $= 0.005/0.253(100) = 1.98\%$

$\eta s = 0.825(1)(0.94)(1)(0.98) = 0.7602$

$Hea = 1341.752 - (0.7602/0.98)(83.029) = 1277.345$

$\Delta Ha = 0.7602(83.029) = 63.116$

Assume a 6th stage efficiency of 80%

Expanding isentropically to 1.7 psia, from the Mollier Diagram
$\Delta H' = 1277.345 - 1198 = 79.345$

$He_7 = 1277.345 - 0.80(79.345) = 1213.869$

$Qe = \nu \dot{e}w = 279.98(0.0564) = 15.791\ ft^3/sec$

$Ns = 90(3.974)/3.915 = 91.356$

$Ds = 1.27$ $\eta_D = 0.847$

$U/Co = 91.356(1.27)/154 = 0.7534$

$U = 0.7534(1993.850) = 1502.167$ ft/sec

since U 1500 set U = 1500 and recompute U/Co

$U/Co = 1500/1993.85 = 0.7523$ and $(U/Co)/(U/C_D) = 0.7523/0.7534 = 0.998$

$\therefore \eta/\eta_D(U/Co) = 1$

$Dia = 1500(720)/\pi(90,000) = 3.82$ inches

$Re^* = 1500(3.82)/12(279.98)(3.2 \times 10^{-7})(32.2) = 1.655 \times 10^5$

$\therefore \eta/\eta_D(Re^*) = 0.96$

from Mach Tables @ $\gamma = 1.3$ and $P_R = P_7/P_6 = 1.7/4 = 0.425$; $M' = 1.210$

$AMR = 0.941(1 - 0.7523)(1.210) = 0.280$

$\therefore \eta/\eta_D(AMR) = 1$

$h/D = 0.15$ $h = 0.15(3.82) = 0.573$ inches

% leakage = 0.005/0.573(100) = 0.874 %

$\eta s = 0.847(1)(0.96)(1)(0.99) = 0.8060$

$Hea = 1277.345 - (0.8060/0.99)(79.345) = 1212.747$

$\Delta Ha = 0.8060(79.345) = 63.954$

$\eta overall = (63.954 + 63.116 + 61.945 + 59.761 + 57.249 + 57.755)/448$

$= 363.780/448 = 0.8120$ or 81.20%

Appendix II

LJUNGSTROM TURBINE

(Radial Outflow)

5 Stage ; 50,000 rpm ; $\psi N = 0.92$; $\psi R = 0.75$; $\alpha = 16^{o}$

Stage No.	1	2	3	4	5
Avg. Dia.	1.954	2.898	3.842	4.786	5.730
Avg. Ut	426	632	838	1044	1250
ΔHs isen	130.00	60.00	75.00	100.00	150.18
ΔHs tot	130.00	69.51	76.20	101.40	152.64
U/Co	0.167	0.339	0.429	0.463	0.452
ηH	0.419	0.647	0.684	0.683	0.684
Cu_3	948.12	132.23	-170.15	-331.62	-352.78
Ca_3	485.34	354.89	371.53	428.64	525.90
C_3	1065.12	378.73	408.68	541.94	633.27
P_2	39	26.5	15.5	7.1	1.7
T_2	992	903	799	657	437
ρ exit	0.0452	0.0327	0.0207	0.0105	0.0032
He	1529.53	1484.56	1432.44	1363.18	1258.77
He'	1454.00	1469.53	1409.56	1332.44	1213.0
ΔHa	54.47	44.97	52.12	69.26	104.41

ηH overall = 325.23/448 = 0.7260 = 72.60%

Chord Length = [[(Dt - Ds)/2] - 9(Ce)]/10 = [[(5.98 - 1)/2] - 9(0.030)]/10 = 0.222

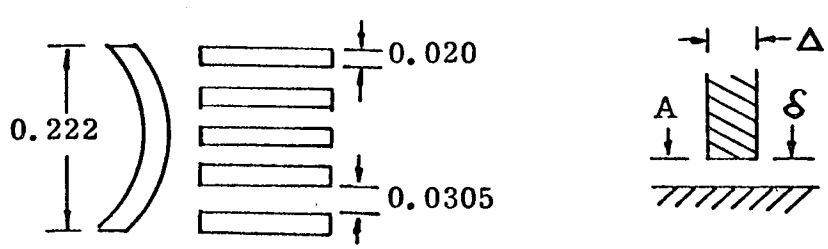

$\Delta = 0.020$ $\delta = 0.002$ $\alpha = 0.97$ $\gamma = 1.00$

Stage No.	1	2	3	4	5
A	0.0123	0.0182	0.0241	0.0301	0.0360
P_n / P_o	0.4351	0.6795	0.5849	0.4581	0.2394
ϕ	0.39	0.33	0.36	0.385	0.41
G	0	0.0037	0.0037	0.0030	0.0018

Windage loss

$HP_d = Kw(\rho/g)(D^2U^3/550)$

$HP_d = [0.001(0.0032)(5.73)^2(1250.1)^3] / (32.2)(144)(550) = 0.081$

$HP_1 = GH(778)/\eta_H(550)$

Stage No.	1	2	3	4	5
HP_1	0	0.485	0.574	0.621	0.559

$\sum HP_1 = 0.485 + 0.574 + 0.621 + 0.559 = 2.239$

1 horsepower

η overall = (0.726)(1)/ 1 + 2.239 + 0.081 = 0.2187

5 horsepower

η overall = (0.726)(5)/ 5 + 2.239 + 0.081 = 0.4959

10 horsepower

η overall = (0.726)(10)/ 10 + 2.239 + 0.081 = 0.5893

LJUNGSTROM TURBINE

(Radial Outflow)

Six Stage ; 50,000 rpm ; $\psi N = 0.92$; $\psi R = 0.75$; $\alpha = 16^{\circ}$

Stage No.	1	2	3	4	5	6
Avg Dia	1.790	2.578	3.366	4.154	4.942	5.730
Avg Ut	390.5	562.4	734.3	906.3	1078.2	1250.1
ΔH_s isen	108.0	50.00	62.47	73.30	83.30	107.83
ΔH_s tot	108.0	57.84	63.53	74.35	85.21	111.36
U/Co	0.168	0.330	0.412	0.470	0.522	0.529
ηH	0.421	0.641	0.681	0.682	0.700	0.700
Cu_3	860.30	145.33	-101.33	-305.55	-516.11	-620.69
Ca_3	442.37	323.73	339.28	367.04	392.93	449.19
C_3	967.37	354.85	354.09	477.58	648.66	766.16
P_2	45	23	15	8.8	4.5	1.7
T_2	1010	936	850	748	625	460
ρ exit	0.0515	0.0277	0.0192	0.0125	0.0070	0.0031
He	1538.53	1501.45	1458.19	1407.48	1347.83	1269.88
He'	1476.00	1488.53	1438.98	1384.89	1324.18	1240.00
ΔHa	45.47	37.08	43.26	50.71	59.65	77.95
ν_2	19.425	36.106	51.955	79.84	143.54	322.11

ηH overall = 314.12/448 = 0.7012 = 70.12%

Chord length for six stage radial flow turbine

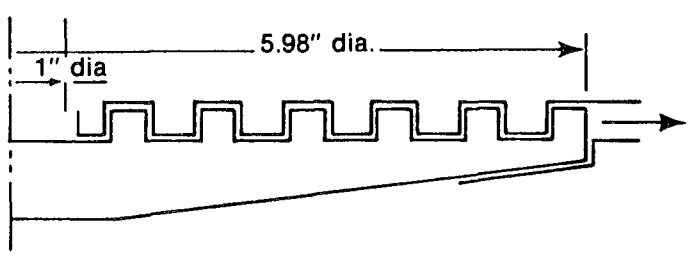

Chord = [[(Dt - Ds)/2] - 11(Cl)] /12 = [[(5.98 = 1.00)/2] - 11(0.030)] /12 = 0.180 inches

XBL 7711-11302

0 0 0 0 4 9 0 1 2 6 1

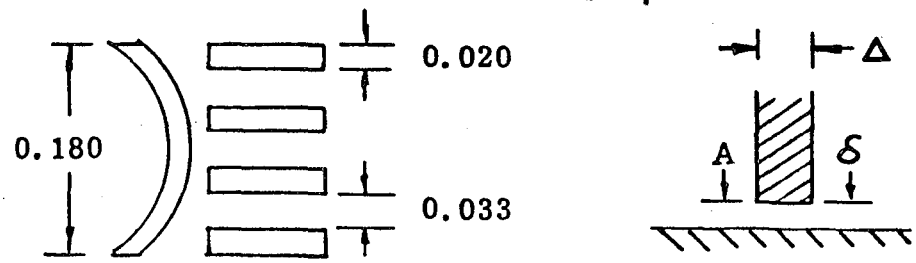

$A = \pi D \delta$ $\alpha = 0.97$ $\gamma = 1.00$ $\Delta = 0.020$ $\delta = 0.002$

Stage No.	1	2	3	4	5	6
A	0.0112	0.0162	0.0211	0.026	0.0311	0.0360
P_n/P_o	0.502	0.511	0.652	0.587	0.511	0.378
ϕ	0.42	0.41	0.37	0.39	0.41	0.435
G	0	0.0046	0.0029	0.0025	0.0019	0.0013

$HP_1 = GH(778)/\eta H(550)$

Stage No.	1	2	3	4	5	6
HP_1	0	0.508	0.376	0.380	0.320	0.283

$\sum HP_1 = 1.867$

$HP_d = 0.001(0.003)/32.2(550)[(5.73/12)^2](1250.1)^3 = 0.076$

1 horsepower

η overall $= (0.7012)(1)/1 + 1.867 + 0.076 = 0.2383$

5 horsepower

η overall $= (0.7012)(5)/5 + 1.867 + 0.076 = 0.505$

10 horsepower

η overall $= (0.7012)(10)/10 + 1.867 + 0.076 = 0.5871$

Appendix III

COEFFICIENT OF PERFORMANCE OF RANKINE SYSTEM

The Rankine cycle system COP was evaluated for the one and four stage axial turbines at 1, 3, 25, and 75 tons refrigeration capacity and for the six stage radial outflow turbine at 1, 3, and 10 tons refrigeration capacity.

The Rankine cycle conditions used for this evaluation were as follows:

Tin max = 1100°F
T evap = 320°F
T cond = 120°F
Drive efficiency, $\eta_D = 1.0$
Feed pump efficiency, $\eta_p = 0.60$
Fuel burner efficiency, $\eta_B = 0.86$
Regenerator temp. differential = 50°F

COP_{VC} for 1 - 3 tons = 3.7
COP_{VC} for $>$3 tons = 4.0

System capacity was converted to shaft horsepower using the equation:

$$hp/ton = 4.715/COP_{VC}$$

At the horsepower values corresponding to the above capacities turbine efficiency for the axial turbines were obtained from Figure 3 and from Table 5 for the radial outflow turbine.

Using these values of turbine efficiency, the values of pump and burner efficiency stated above and the cycle conditions, the Rankine cycle efficiency at various refrigeration capacities was obtained from the equation:

$$\eta_{RC} = [\eta_t \Delta h' - \Delta h_p] / [(\Delta h/\eta_B) + \Delta h_s - \Delta h_R - \Delta h_p] \quad \text{and}$$

$$\Delta h_p = (Psat - Pcond)(144)/(\rho cond)(778)\eta_p$$

where:
- η_t = turbine efficiency
- $\Delta h'$ = isentropic head drop across the turbine
- Δh = enthalpy change of superheated vapor
- Δh_s = enthalpy change from saturated liquid @ 120°F to saturated vapor @ 320°F
- Δh_R = enthalpy change in regenerator
- Psat = evaporator pressure
- Pcond = condenser pressure
- ρcond = density of saturated liquid in condenser
- η_p = pump efficiency

η_B = fuel burner efficiency

Δh_p = enthalpy change across the feed pump

These Rankine cycle efficiencies were then used in the following equation to determine the coefficient of performance of the Rankine system as a function of refrigeration capacity.

$$COP_{RV} = \eta_{RC}\, \eta_D\, COP_{VC}$$

The values of COP_{RV} and η_{RC} for the three turbines were then plotted as a function of system capacity. This plot is shown in Figure III-1.

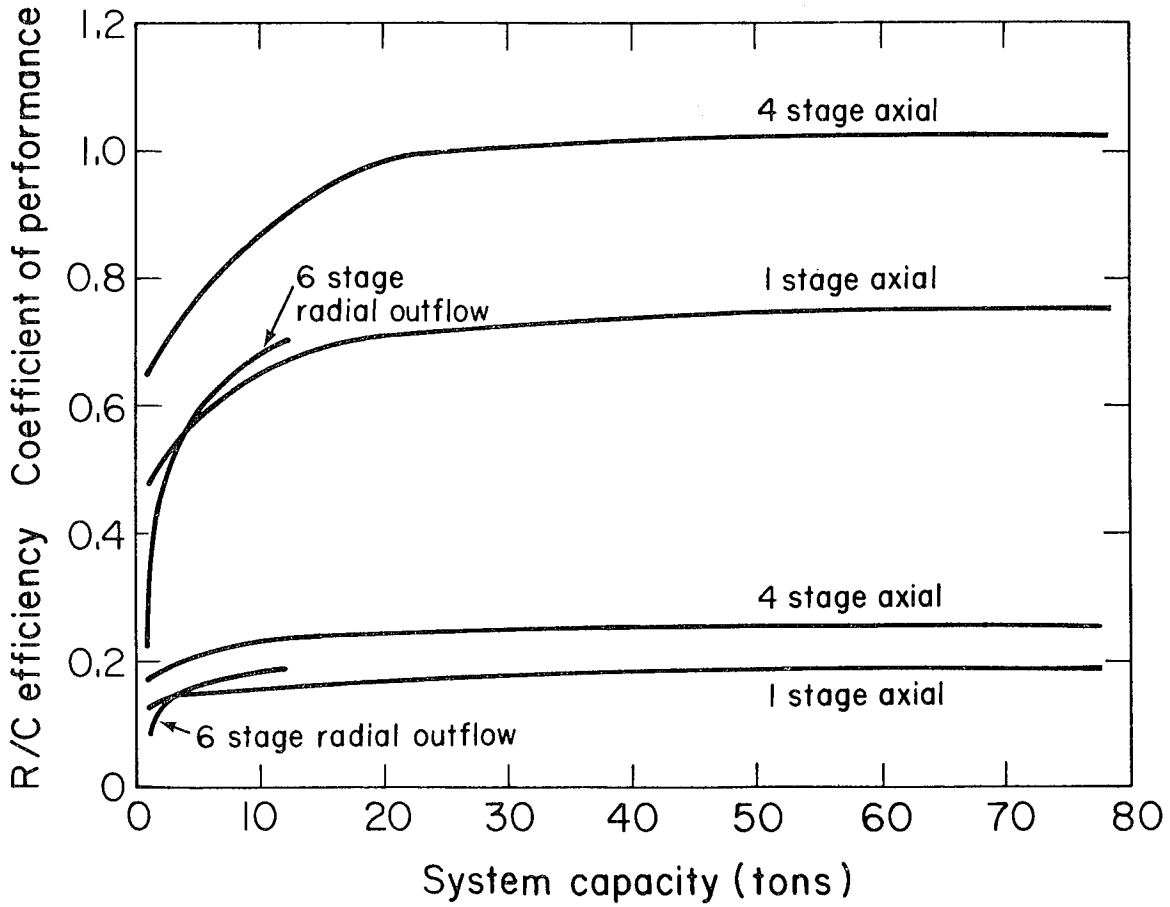

XBL7711-11302A

Fig. III-I Comparison of Coefficient of performance Rv and η R/C for Solar Powered Refrigeration Machines

Appendix IV

VAPOR COMPRESSOR OPERATING CHARACTERISTICS

A preliminary evaluation of performance and size for a high speed single stage vapor compressor was completed. The compressor was sized for capacity and speed consistant with nominal turbine design conditions established in this report. The performance evaluation utilized a 45°F evaporator and 120°F condenser and the air conditioning cycle working fluid was selected depending on capacity and desired compressor speed characteristics.

Figures 1 and 2 present results of this evaluation for cooling capacities up to 15 tons. The analysis involved calculating compressor specific speed (based on exit volume flow) to determine optimum achievable efficiency. Loss factors were then estimated based on compressor size (Reynolds number effects) and impeller tip speed (rotor tip Mach number). Also shown in Figure 1 is the efficiency of a single stage 3 ton compressor designed and tested by Barber-Nichols.

Similar analysis at greater capacity showed that R-12 could be selected to yield acceptable centrifugal compressor design parameters in the range of compressor speed of 50,000 to 90,000 rpm. A detailed analysis of specific applications would be needed to optimize turbo compressor speed for peak system performance. Results of this analysis do indicate, however, that the speeds and power levels selected for the turbine analysis yield reasonable compressor design parameters for the cases examined.

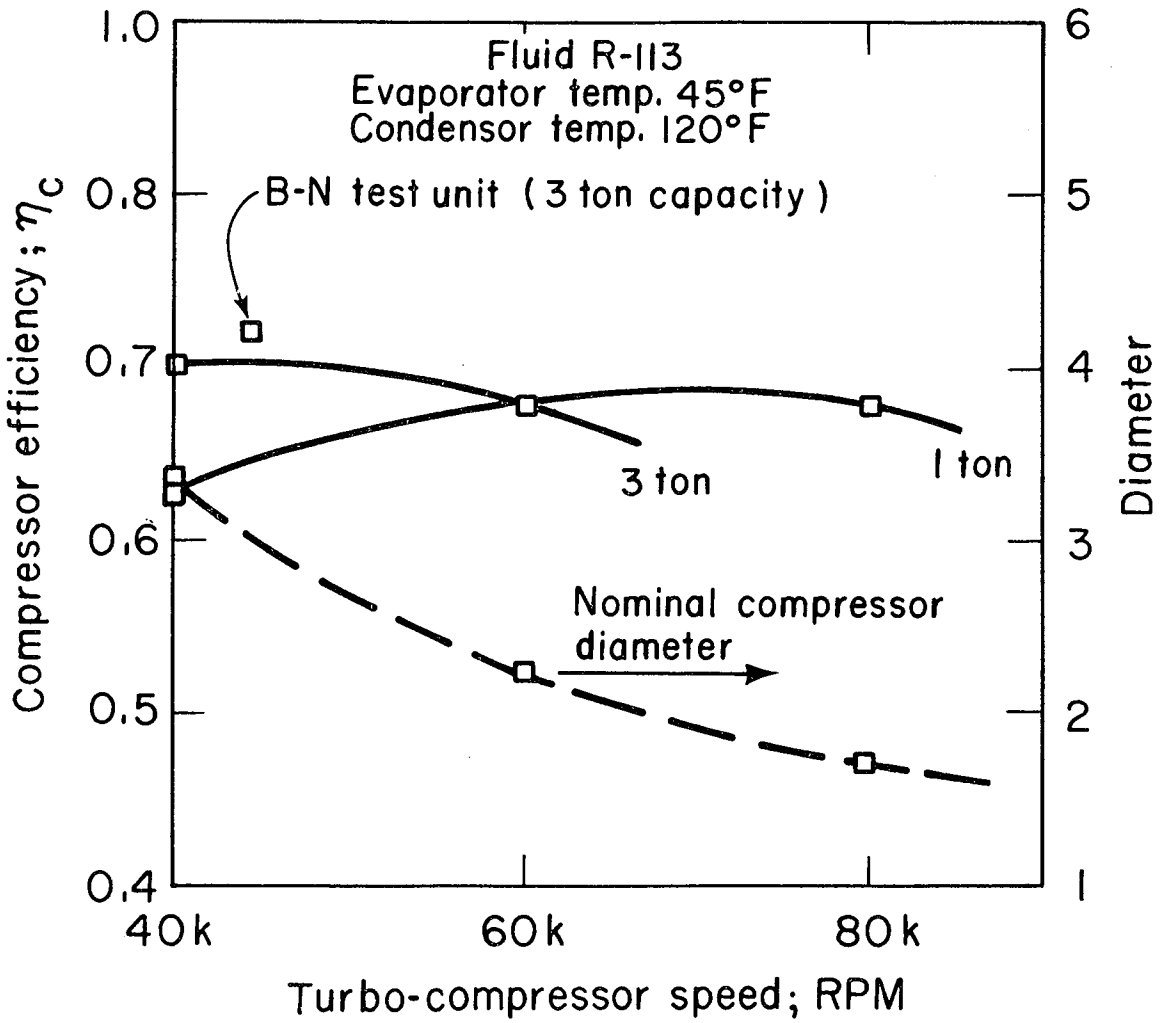

XBL7711-11305

Fig. IV-1 High Speed Compressor Characteristics at Low Cooling Capacities

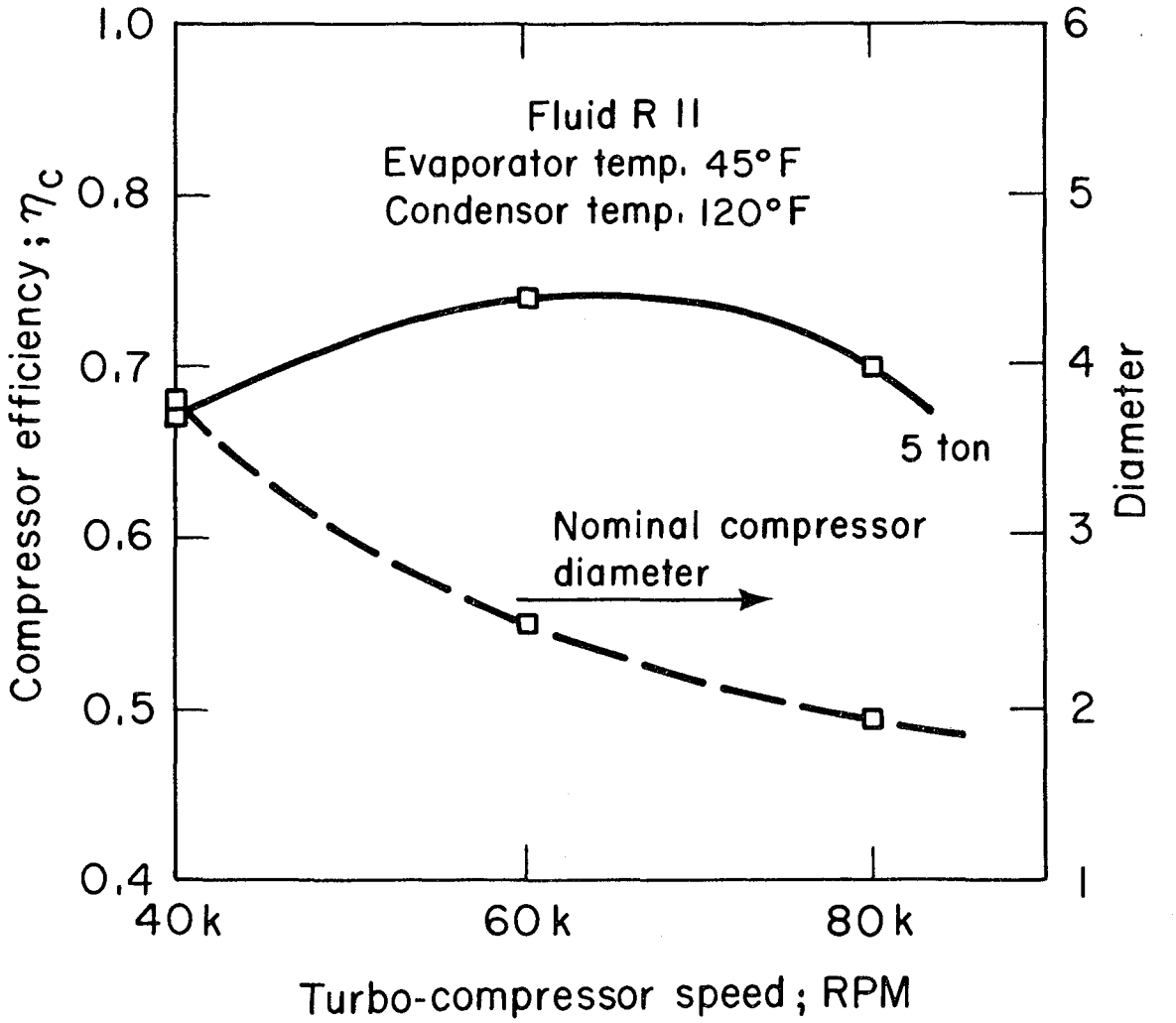

XBL 7711-11301A

Fig. IV-2 High Speed Compressor Characteristics at Low Cooling Capacities

This report was done with support from the United States Energy Research and Development Administration. Any conclusions or opinions expressed in this report represent solely those of the author(s) and not necessarily those of The Regents of the University of California, the Lawrence Berkeley Laboratory or the United States Energy Research and Development Administration.

0 0 0 0 4 5 0 2 2 9 4